A Heuristic Nonlinear Constructive Method for Electric Power Distribution System Reconfiguration

Thomas E. McDermott

Dissertation submitted to the Faculty of the Virginia Polytechnic Institute and State University in partial fulfillment of the requirements for the degree of

Doctor of Philosophy
in
Electrical Engineering

Robert P. Broadwater, Chair
Walling Cyre
Terry Herdman
Yilu Liu
Hugh VanLandingham

April 23, 1998
Blacksburg, Virginia

Keywords: Discrete Ascent Optimal Programming, Load Restoration, Losses, Optimization Methods, Power Distribution Control, Power Distribution Planning, Power System Restoration

A Heuristic Nonlinear Constructive Method for Electric Power Distribution System Reconfiguration

Thomas E. McDermott

(ABSTRACT)

The electric power distribution system usually operates in a radial configuration, with tie switches between circuits to provide alternate feeds. The losses would be minimized if all switches were closed, but this is not done because it complicates the system's protection against overcurrents. Whenever a component fails, some of the switches must be operated to restore power to as many customers as possible. As loads vary with time, switch operations may reduce losses in the system. Both of these are applications for reconfiguration.

The problem is combinatorial, which precludes algorithms that guarantee a global optimum. Most existing reconfiguration algorithms fall into two categories. In the first, branch exchange, the system operates in a feasible radial configuration and the algorithm opens and closes candidate switches in pairs. In the second, loop cutting, the system is completely meshed and the algorithm opens candidate switches to reach a feasible radial configuration. Reconfiguration algorithms based on linearized transshipment, neural networks, heuristics, genetic algorithms, and simulated annealing have also been reported, but not widely used. These existing reconfiguration algorithms work with a simplified model of the power system, and they handle voltage and current constraints approximately, if at all.

The algorithm described here is a constructive method, using a full nonlinear power system model that accurately handles constraints. The system starts with all switches open and all failed components isolated. An optional network power flow provides a lower bound on the losses. Then the algorithm closes one switch at a time to minimize the increase in a merit figure, which is the real loss divided by the apparent load served. The merit figure increases with each switch closing. This principle, called discrete ascent optimal programming (DAOP), has been applied to other power system problems, including economic dispatch and phase balancing. For reconfiguration, the DAOP method's greedy nature is mitigated with a backtracking algorithm. Approximate screening formulas have also been developed for efficient use with partial load flow solutions. This method's main advantage is the accurate treatment of voltage and current constraints, including the effect of control action. One example taken from the literature shows how the DAOP-based algorithm can reach an optimal solution, while adjusting line voltage regulators to satisfy the voltage constraints.

Acknowledgements

I thank the Electric Power Research Institute for supporting development of the DEWorkstation, which made this research possible.

Special thanks are due to my wife, Kathleen Retcofsky McDermott, for her patience and understanding during my pursuit of this degree.

Contents

List of Figures

List of Tables

Chapter 1

Introduction

The electric power distribution system delivers power to the customers from a set of distribution substations. While the transmission and subtransmission lines are configured in a meshed network, the distribution feeders are configured radially in almost all cases. This radial configuration simplifies overcurrent protection of the feeder. To help restore power to customers following a fault, most feeders are provided with tie circuits to neighboring feeders from either the same or different substations. A number of switching operations are needed to restore power using these ties.

Loads vary with time of day, day of the week, and season. Each type of load (residential, commercial, industrial) has a different time profile, and each feeder serves a different mix of loads. Therefore, the load pattern on each feeder varies constantly, and with a different variation on each feeder. This creates an opportunity to constantly keep losses at a minimum by reconfiguring the feeders during the day. Automatic switches and control systems must be installed to perform this distribution automation, at a cost that must be balanced against the savings in losses.

The distribution system should be operated at minimum cost, subject to a number of constraints:

1. radial configuration

2. all loads are served

3. overcurrent protective devices are coordinated

4. lines, transformers, and other equipment within current capacity limits

5. voltage drop within limits

Reconfiguration is the process of operating switches to change the circuit topology so that operating costs are reduced, while still meeting the constraints listed above. For the distribution system, the cost to be minimized is essentially the cost of losses, and the losses are essentially a quadratic function of the line currents. There may be other costs to consider in the reconfiguration analysis, such as the cost to operate or install switches.

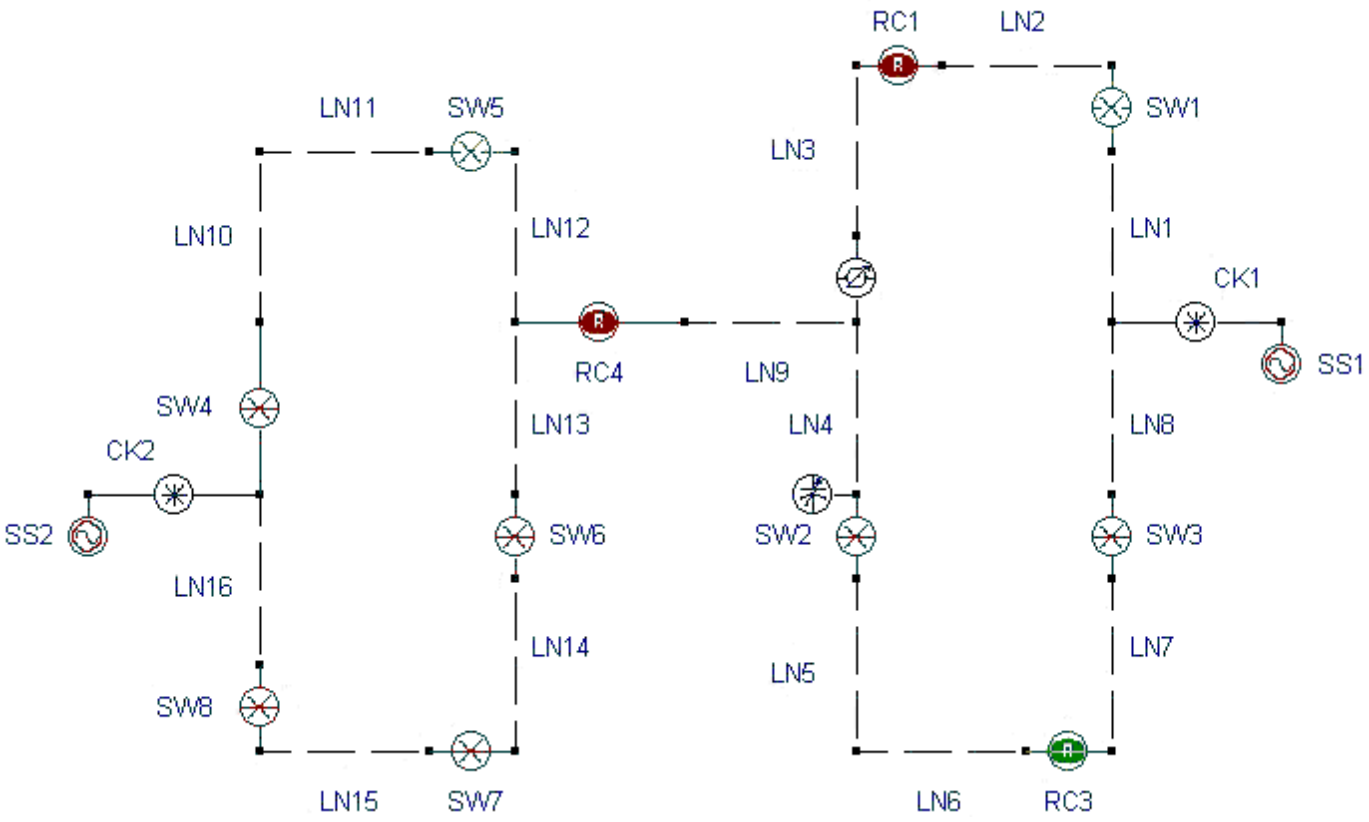

Figure 1.1 - A simple distribution system.

Figure 1.1 shows a distribution system with two sources and several switching devices. SW1, SW5, and RC3 are open so that the system is operating radially. The ending loads in feeder segments LN2 and LN6 are some distance from their source, SS2. To correct for possible voltage drop problems at these ending loads, it's typical to use capacitor banks, as illustrated between LN4 and SW2, or voltage regulators, as illustrated between LN3 and LN9. The capacitor banks may be of fixed size, controlled locally by temperature or time of day, or controlled remotely. Voltage regulators are usually controlled locally. For the system operating as shown in Figure 1.1, it's likely that losses could be reduced by transferring some of the load from source SS2 to source SS1. For example, RC3 might be closed and then SW2 opened, transferring the loads in LN5 and LN6 from SS2 to SS1. Analyzing these options is the subject of a reconfiguration algorithm.

Since a typical distribution system would have hundreds of switches, a combinatorial analysis of the options (2^m) could easily take too long. Also, the analysis and application of the constraints takes more time and complicates the use of classical optimization techniques. However, the potential cost savings increase dramatically as the number of switches increases [Willis et. al., 1996], so it is important for the analysis method to handle large systems.

Reconfiguration may be considered in two different situations. First, in the system planning or system design stage, the normal operating configuration and switch placement can be adjusted to achieve a minimum cost system. Capital and maintenance costs of new switches must be considered along with the cost of losses. Second, in the real-time operation mode, the protective system may have operated during a fault to reconfigure the system. In this new configuration, it would be useful to examine switching operations that might reduce losses while not disconnecting any more customers. Here, the cost and the time involved in operating switches must be considered along with the cost of losses.

The two situations differ in other ways, too. In the real-time mode, reconfiguration analysis must be very quick, and it starts with an existing radial system. In the planning or design mode, the analysis could take longer if it is more thorough, and also more of the system could be considered a blank slate.

1.1 Effect of Constraints on Reconfiguration

One of the major constraints on reconfiguration is that the network must not have any loops. Some of the general optimization algorithms have difficulty enforcing this radial constraint directly. This is a particular problem for reconfiguration, because a meshed network with all switches closed will have minimum losses, but that violates the radial constraint. A method that builds the network from scratch can easily enforce the radial constraint, simply by not closing any switches that form a loop.

The other major constraint on reconfiguration is the limit on line capacity or voltage drop. These constraints are closely related, because a line carrying current close to its thermal capacity will also have a larger resistive voltage drop. Heuristically, solutions with a good voltage profile are more likely to have low losses and line currents within limits. In a given situation either the voltage or the current constraint may be reached first.

Current constraints can be alleviated by switching, or in the longer term, by re-conductoring the feeder or installing a larger substation transformer. Voltage constraints can be alleviated by switching or installing capacitor banks, or by adjusting voltage regulators. Secondarily, capacitor banks and voltage regulators can reduce line currents and thus may help to alleviate current constraints.

For example, suppose the last load in Figure 1.2 can be served by closing either switch A or B. Switch A produces minimum losses, but violates the voltage drop constraint because its feeding path is already heavily loaded. Therefore switch B is closed to serve the last load. In most design processes, capacitor banks and voltage regulators will then be adjusted on the reconfigured network to improve the voltage profile. After the capacitors and regulators have operated, switching operations that were previously discarded due to constraints may become feasible. For example, by switching on the capacitor in Figure 1.2, it might be possible to close switch A instead of B, without violating the voltage constraint.

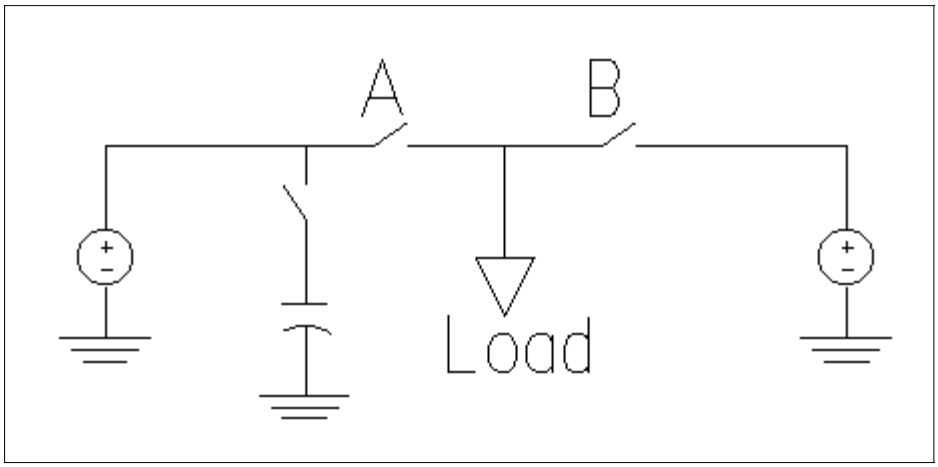

Figure 1.2 - Capacitor switching can alleviate voltage constraints during reconfiguration.

1.2 Problem Statement

The objective of this dissertation is to develop an efficient reconfiguration algorithm that directly constructs an optimal solution for minimum losses, accounting for constraints. The reconfiguration should consider capacitor and voltage regulator control along with switching operations. The algorithm should also isolate any failed components, and restore power to as many customers as possible.

Chapter 2

Summary of Previous Work

The only method known to produce a guaranteed optimal reconfiguration is "branch and bound" [Boardman, 1985]. This amounts to an exhaustive search, except that a search direction will be terminated when it becomes obvious that its end result will be less optimal than a previously found solution. Branch and bound will work better if the initial solution is close to optimal, because more pruning will occur. Branch and bound also benefits from breaking the problem into subproblems, each of which can be optimized separately. Even so, branch and bound is a combinatorial method and hence too slow for practical use.

Therefore, most of the recent work on reconfiguration has used either a branch exchange method or sequential switch opening method. Heuristics are applied in most cases to reduce the number of switching options considered. Even so, approximate loss formulas, linearized costs, and other simplifying assumptions are typically used to avoid repetitive solution of system load flows. Attempts have also been made to use neural networks, genetic algorithms, and simulated annealing solutions for the reconfiguration problem.

2.1 Branch Exchange Methods

Branch exchange starts with a feasible solution - the distribution network operating in a radial configuration. One of the tie switches is closed, and then another switch is opened in the loop created, which restores a radial configuration. The switch pairs are chosen through heuristics and approximate formulas for the change in losses. The branch exchange process is stopped when no more loss reductions are available.

As developed by [Civanlar, 1989], this method requires a full system load flow analysis at the current operating condition. The change in losses effected by operating a pair of switches is estimated from:

$$\Delta P = \mathrm{Re}\left\{2\left(\sum_{i\in D} I_i\right)(E_m - E_n)^*\right\} + R_{loop}\left|\sum_{i\in D} I_i\right|^2 \tag{2.1}$$

For the sample system in Figure 1.1, to analyze a possible exchange of RC3 and SW2, the resistance R_{loop} would be the series resistance of LN8, 7, 6, 5, 4, 9, 13, 14, 15, and 16. E_m and E_n are the resistive components of the voltage drop from source to bus on each side of the switch to be opened, RC3. E_n is defined on the load-transferred-from side of the switch to be opened, or the SS1 side of RC3. Therefore, the losses are predicted to decrease when $E_n > E_m$, or when load is transferred from the higher voltage drop side of the open switch. The transferred load is represented by ΣI_i, the sum of the load currents in LN5 and LN6. After the switch operation, the system load flow is solved again to analyze the next switch exchange.

This method is very fast and good for use in real-time operations. Even though it is easily trapped in a local minimum, it can be used to provide a loss reduction after an emergency reconfiguration. The method can be used with the total number of switching operations limited to some number that reflects crew availability and switching time.

A variation on the branch exchange method has been used in Japan, where the density of automatic switches is evidently rather high. Aoki defines an "arc" as a segment between two branch points; it usually has several automatic switches along its length. On an open loop, the arc containing the tie point is moved in one direction or the other. Then, a continuous piecewise quadratic problem is solved to determine the point on the arc where the break should occur. This solution is then rounded to the nearest actual switch location.

2.2 Loop Cutting Methods

The loop cutting or sequential switch opening method [Shirmohammadi, 1989] starts with all tie switches closed. The typical distribution system would be "weakly meshed" in this state, compared to the transmission system. A load flow of the meshed system will provide a minimum-loss solution (in the absence of any control action). However, the system must be brought into a radial configuration. This is done by opening switches that carry the least current, on the premise that these will least disturb the meshed load flow solution. After each switch opening, the meshed load flow is solved again before selecting the next switch to open. The algorithm stops when the system is radial.

For the sample system in Figure 2.1, all three switches A, B, and C would be closed initially. If switch C were opened first, switch B could not be opened without isolating some of the load, and vice versa. The number of weakly meshed load flows that must be performed is usually low, at most two in the case of Figure 2.1.

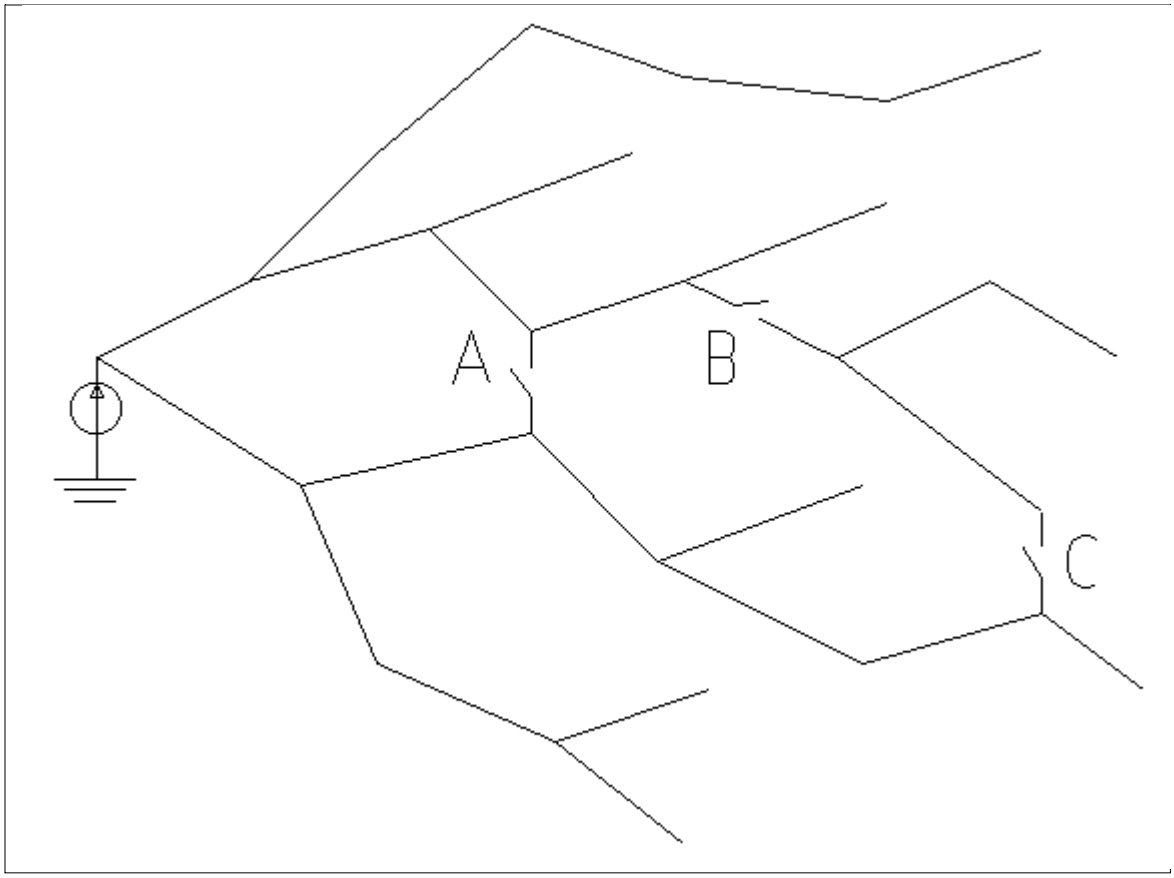

Figure 2.1 - A weakly meshed distribution network.

2.3 Heuristic Search Methods

Search methods involve building the network in stages, or analyzing a decision tree of switching operations, using a depth-first or best-first algorithm. The best-first algorithm is sometimes called a "greedy" search. The greedy search cannot ensure a global optimum, though use of an adjustable number of wrong steps has been investigated for reconfiguration [Carrillo-Caicedo, 1995]. Branch and bound is the broadest search algorithm, but various heuristics have been applied to make its running time reasonable for reconfiguration [Hsu, Morelato, Taylor]. Heuristics represent the application of engineering judgment without detailed analysis of each alternative, so they are desirable in any algorithm.

2.4 Transshipment

The linearized transshipment method [Glamocanin 1990] is most closely related to the method presented in this dissertation. The network starts with just the distribution substations, and the feeder segments are switched in one at a time. Of the segments available to switch in, the one with minimum unit transshipment cost is chosen first. Then, of the other segments available to

serve that new load point, the chosen segment is checked to make sure it results in the minimum increase in losses. The increase in losses for each switching is an approximate quadratic formula. The algorithm stops when all loads are served; the system is kept radial as the segments are switched in. It is also a greedy search.

The transshipment cost was linearized to the feeder resistance multiplied by maximum current capacity. Figure 2.2 shows the I-squared R power loss for two feeders of different capacity, along with linear approximations through the points of maximum current. The linearized transshipment cost defines these straight lines. For feeder 1, the linearized transshipment cost is 10 amps multiplied by 1.5 ohms, or 15. For feeder 2 the linearized cost is 15 amps multiplied by 0.7 ohms, or 10.5. Thus feeder 2 has the lowest cost per unit ampere, but its cost relative to feeder 1 is greater than the simple ratio of resistances. Note that the transshipment cost does not depend on the actual load current nor on any other operating condition.

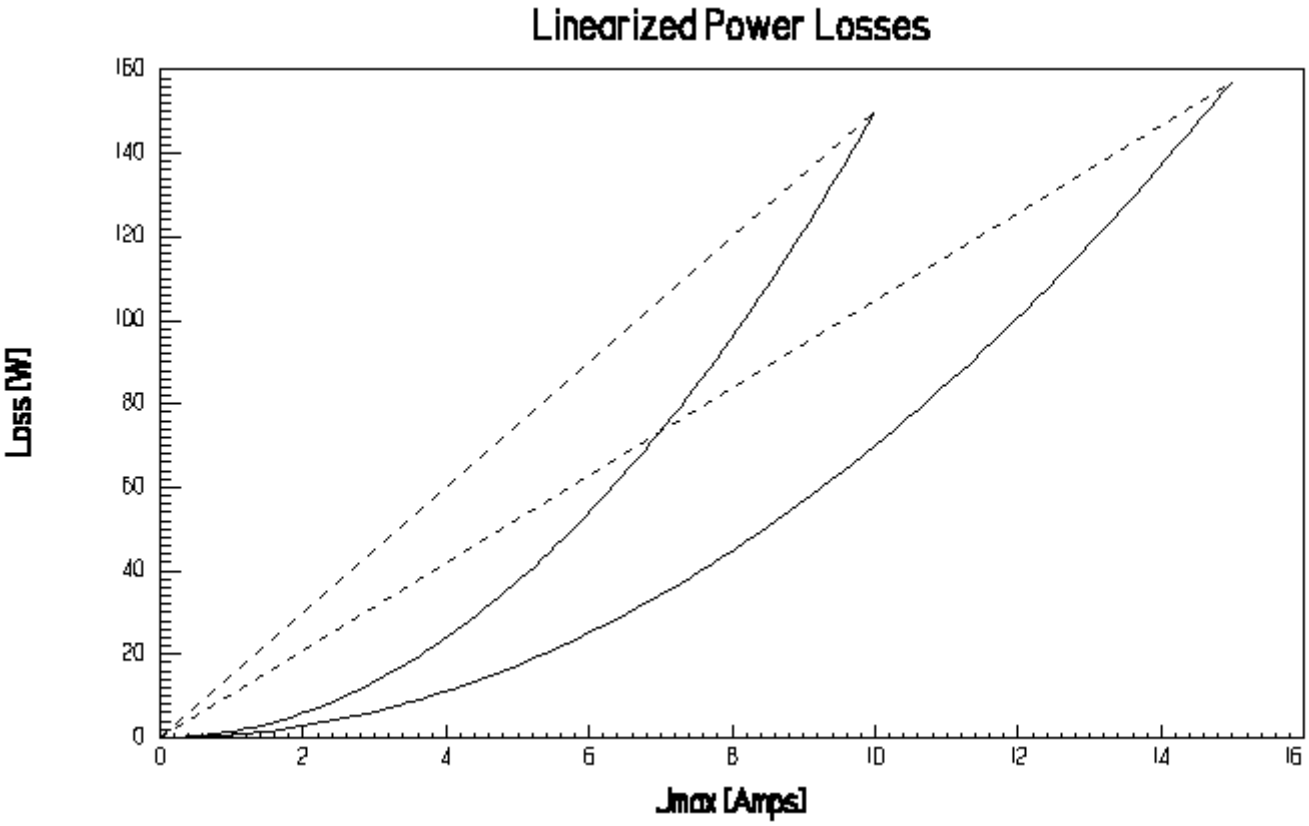

Figure 2.2 - Linearized feeder transshipment costs.

The two-stage comparison feature is important. If the segment that results in minimum loss is chosen at each step, the tendency will be to add the smallest loads first, using the best feeder segments. Obviously this will not lead to an optimal or even a good solution. In a discussion of

Glamocanin's paper, Baldick showed this problem for the simple system shown in Figure 2.3. Adding the minimum loss segment at each step resulted in feeders 1-2-3 and 1-4, with total losses of 6.25 kW. In his closure, Glamocanin showed that his transshipment method produced the optimal solution of one feeder, 1-2-3-4, with losses of 5.25 kW. He also recommended that feeder reconfiguration and capacitor placement be solved as separate problems in any case.

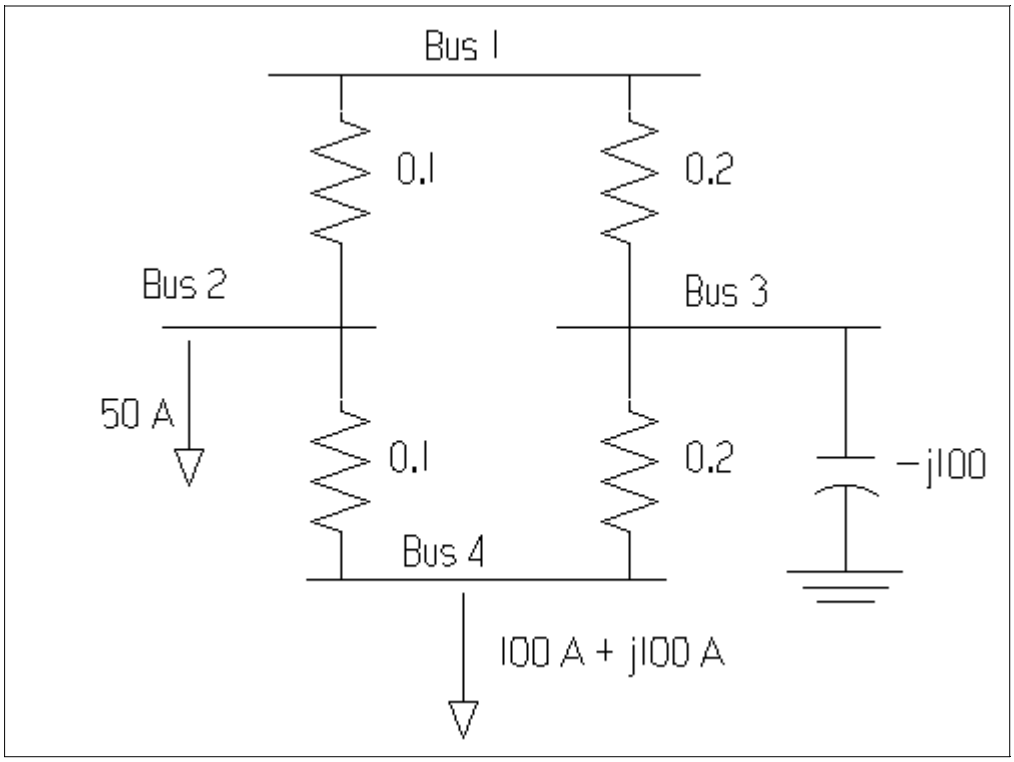

Figure 2.3 - Baldick's problem with shunt capacitor banks.

The transshipment problem can be solved with linear programming techniques. However, the linear transshipment cost is an approximation for distribution networks. If there are fixed costs, these must be ignored. Further, the solution from a general transshipment algorithm may not be radial [Wall].

2.5 Simulated Annealing

Simulated annealing is not a reconfiguration algorithm by itself, but is a modification to some other basic algorithm [Chang, Sarfi]. Its purpose is to avoid being trapped in local minima, by not always taking the best choice at each step. Under simulated annealing, a random choice is accepted with a probability that decreases exponentially with each iteration. Simulated annealing has more potential to find the global optimum, though this can't be proven. It is readily applied on decision tree or branch exchange methods, by adding an extra outer loop to the basic algorithm.

Because of the extra analysis time, simulated annealing is more applicable to planning rather than operations.

2.6 Genetic Algorithms

Genetic algorithms have become very popular as a method of finding global optimums. As applied to reconfiguration [Nara], the switch states are encoded in strings of 0/1 "chromosomes", and a population of, for example, 50 topologies is built at random. At each iteration, two parent topologies are selected at random for crossbreeding, which is a process of combining the chromosomes according to some defined algorithm. Then mutation, a random alteration of some chromosomes, may occur with a certain probability. If the resulting child is better, it replaces an existing topology in the population of 50. This process of crossbreeding continues for a number of iterations. The population also has to be re-seeded periodically with random strings to avoid inbreeding. As the population evolves, there will always be a best solution that should steadily improve.

Genetic algorithms are most attractive for parallel processing environments, and when each child can be evaluated quickly. The crossbreeding and mutation algorithms must be custom designed and tested for each application. Parameters such as the number of crossbreedings per generation, mutation probability, number of generations, population size, and percentage of population reseeded must all be determined by testing. Applications to reconfiguration have used simplified network analysis because many thousands of topologies are considered, so the resulting solution may not be optimal with a more detailed model. The method presented in this dissertation uses more comprehensive analysis with fewer iterations.

2.7 Neural Networks

Neural networks have been applied to recognize a load pattern from feeder measurements and other data, then select a pre-analyzed topology and switching strategy to reconfigure the network for loss reduction [Hayashi, Kim]. It's necessary to discretize load levels and combine similar topologies, otherwise the training sets become too large. The neural network serves as a state estimator but doesn't analyze the topologies, so this method is not really applicable to the problem statement.

2.8 Discrete Ascent Optimal Programming

Discrete ascent optimal programming (DAOP) has been applied to optimal load flow and phase balancing for distribution systems [Dolloff]. In DAOP, the load is picked up in step increments, with each step added at the ending node that will produce the smallest increase in total losses. At each step the loss will increase in discrete increments, hence the name "discrete ascent" optimal programming. DAOP is essentially a greedy algorithm, although it was proved to converge to the global optimum in the case with 3 substations and no constraints.

In this thesis, the DAOP method is extended to the reconfiguration analysis problem. This method provides advantages similar to the linearized transshipment algorithm, but with more accurate load flow analysis. Rather than increment load in steps, the network size is incremented in steps of one switching operation. At each step, each candidate switching operation is evaluated from the increase in loss, divided by the switched segment's apparent load power. This measure is similar to the linearized transshipment cost, except that it includes nonlinear load flow analysis. Capacitor switching and voltage regulator operation have to be considered as part of the reconfiguration problem, and this is another improvement over the transshipment method.

Since DAOP is a greedy search, it cannot be assured of reaching the global optimum except in simplified or special cases. The minimum loss problem is quadratic or piecewise quadratic, so one might expect that with no constraints, DAOP would converge to a global optimum. However, as switches are closed in a DAOP algorithm, certain subsequent switch closings will be ruled out by the radial constraint. Even when all voltage and current limits remain satisfied, the DAOP algorithm will encounter constraints. One of the examples used in Dolloff's thesis shows how a pure DAOP reconfiguration algorithm can be trapped in a local minimum. A backtracking scheme, described in sections 3.6 and 3.7, was developed to address this issue.

Chapter 3

Reconfiguration Algorithms

This chapter describes how a reconfiguration algorithm was implemented in the Distribution Engineering Workstation (DEWorkstation), funded by the Electric Power Research Institute (EPRI). Sections 3.1 and 3.2 describe the advantages of using DEWorkstation for the implementation, and some of the platform-specific issues encountered. The algorithm's features include:

1. isolating failed components (Section 3.3)

2. loss minimization by a properly selected merit figure (Section 3.4)

3. accelerated solution using approximate loss evaluation of candidate switch closings (Section 3.5)

4. backtracking to avoid local minima (Section 3.6)

Section 3.7 walks through an example of the algorithm's main features. Chapter 4 describes several test cases obtained from the literature, and Appendix A contains user instructions for running the application in DEWorkstation.

3.1 DEWorkstation Platform

The reconfiguration algorithm based on DAOP was implemented and tested in EPRI's DEWorkstation [Broadwater, 1995]. The DEWorkstation includes a system model based on graph edges, rather than separate buses and branches. This model organization affects the design of applications for DEWorkstation, and the reconfiguration algorithm takes advantage of component traces built into DEWorkstation:

1. forward and backward component traces

2. feeder path component traces back to the source

3. pointers to components in adjacent circuits

4. brother pointers that identify downstream components fed by this component

The DEWorkstation executive maintains these traces, along with a database and graphical interface. The reconfiguration algorithm uses other applications in DEWorkstation, in particular the radial and network power flow calculations. This architecture saves development time and improves the consistency of results.

Figure 3.1 shows a sample circuit in DEWorkstation, with components numbered in a forward trace starting from the source. The numbering is not unique, but must follow one rule – whenever a component is numbered, all downstream components must be numbered before any others. From the faulted component in Figure 3.1, the feeder path trace would be 4-3-2-1. Some components have pointers to adjacent circuits. In Figure 3.1, only component 7 would have a pointer to the adjacent tie switch. A component's brother pointer jumps to the next forward trace position that doesn't have that component in the feeder path. Figure 3.1 lists the brother for each component in the sample circuit (0 implies a NULL pointer). The brother pointer is useful in finding branches, and summing loads served by a switch.

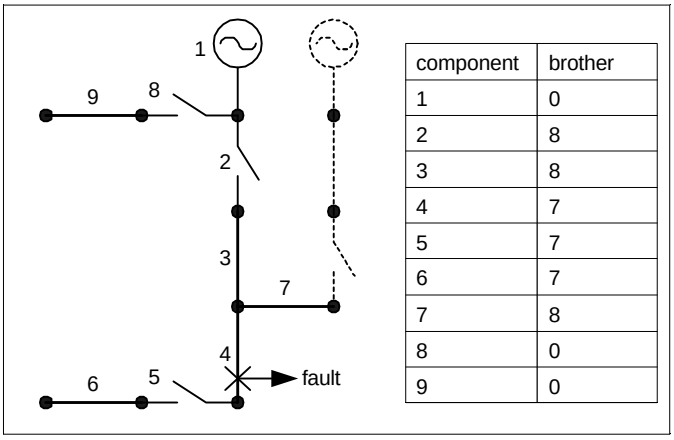

component	brother
1	0
2	8
3	8
4	7
5	7
6	7
7	8
8	0
9	0

Figure 3.1 - Faulted circuit with DEWorkstation component numbering

The DEWorkstation includes a comprehensive database and schematic editor for the distribution system model, with a suite of applications to run against the model. The reconfiguration algorithm calls the following DEWorkstation applications while executing:

1. radial load flow

2. network load flow

3. load estimation

This architecture makes the full analysis capability of DEWorkstation available to the reconfiguration algorithm. In particular, unbalanced loads, regulator control action, and capacitor bank control are accounted for without making approximations in the reconfiguration algorithm. In other reconfiguration algorithms, these effects are often ignored. Results are consistent between applications; the user will not run the reconfiguration algorithm, and then find that DEWorkstation's load flow program gives a different answer.

The load flow calculations in DEWorkstation may be run on the entire system, or on a selected circuit. The reconfiguration algorithm runs most of its load flows on just one circuit at a time, which saves execution time.

3.2 Operating Switches in DEWorkstation

The user may have specified that certain switches may not be operated, either by specifying types of switches, or selecting individual switches. Before attempting to minimize losses, any failed components are isolated by opening switches according to the procedure in section 3.3. All of these switches are marked as inoperable for the reconfiguration algorithm. They are excluded from the opening and closing sequences described in this section, and the automatic sequences described in sections 3.4 through 3.6.

The reconfiguration algorithm needs to open and close switches automatically. DEWorkstation can create loops by closing switches that have one line segment connected to each end, and no other components connected. This allows DEWorkstation to solve a network power flow, and the reconfiguration algorithm uses this to provide a lower bound on the system losses. Once a loop has been created, the switch that was closed to create the loop must be opened before any other switch in that loop is opened. The reconfiguration algorithm needs to account for these switching restrictions, in order to successfully open and close all switches in the system.

Before the optimization process begins, all operable switches must be opened in two passes. First, all of the loop switches are opened. From the DEWorkstation data schema [EPRI], loop switches are identified by checking the flag *pCmp->sCtCmp !*= 0. Second, all remaining operable switches are opened.

To perform a network power flow, all operable switches must be closed. As discussed above, only certain switches may be closed to create loops. The sequence of switch closings is done in two passes. First, all of the operable switches that could not possibly create a loop are closed. These ineligible loop switches meet one of the following two conditions:

1. either end has more than one component connected to it

2. one of the ends does not have a line segment connected to it

In the second pass, all remaining operable switches are closed.

This process does not guarantee that all operable switches can be closed. Some system configurations may not have an eligible loop closing switch for every loop. In those cases, the user could insert zero-impedance line segments to create valid loop switches, without changing the model results. DEWorkstation does not allow nested loops; this case does not have a workaround. The two-pass closing process does tend to maximize the number of loops closed, and it closed all possible loops in the chapter 4 test cases.

3.3 Isolating Failed Components

One of the first steps in reconfiguration is to isolate faults by opening and locking switches. Figure 3.2 shows the algorithm used. Referring to the example in Figure 3.1, a feeder path trace from 4 would find the switch at 2, and lock it open. The forward trace stop point is then set at 8.

The forward trace from 2 will find the switch at 5, lock it open, and then jump to 7. At that point, the adjacent tie switch would be locked open. The trace stops at 8, without opening the switch at 8.

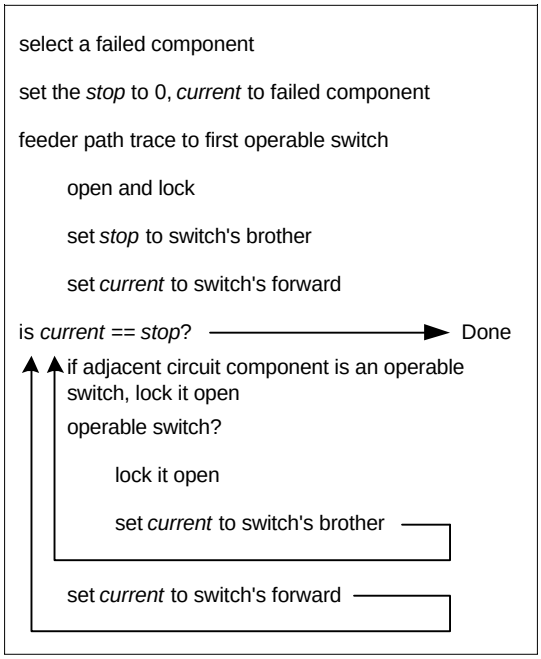

Figure 3.2 - Algorithm to isolate failed components

3.4 Reconfiguration with Full Load Flow Evaluation

Figure 3.3 shows the main reconfiguration algorithm based on DAOP, assuming a full load flow evaluation of candidate switch operations. The user can specify the types of switches to use, and manually lock selected switches through the interface. The fault isolation process may lock more switches. At the end of this process, the algorithm will have a list of operable switches for reconfiguration. The benchmark losses and unserved load are solved with these operable switches in their current state. It's also useful to perform a network load flow with all operable switches closed. This condition provides a lower bound on the losses.

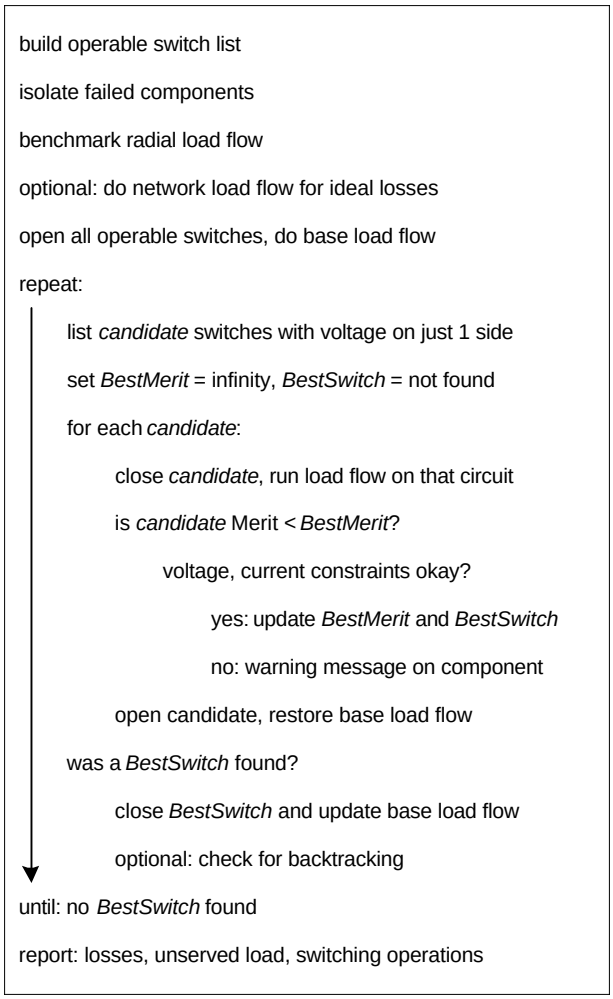

Figure 3.3 - Reconfiguration algorithm with full load flow screening

The reconfiguration starts by opening all operable switches, and then building a list of candidate switches at each step. The candidates must have voltage on just one side of the switch. At each step, all candidates are closed one at a time and the merit figure is evaluated. The candidate with minimum merit figure is closed at that step, and the base case is updated. The total losses increase at each step, according to the discrete ascent nature of the algorithm.

$$M = \Delta P_{loss} / (\Delta S_{load} + 0.001 \Delta Q_{cap}) \tag{3.1}$$

ΔP_{loss} is the incremental loss caused by the candidate switch closing, ΔS_{load} is the load kVA picked up, and ΔQ_{cap} is the utility capacitor bank kVAR picked up.

The merit figure favors minimum loss increment, normalized by the total apparent load picked up, at each step. The normalization could be done equally well using load current magnitude, but normalizing by the real load biased the solution in some cases, as described in section 4.6. Equation (3.1) includes utility-owned capacitor banks as a low-weighted special case, even though they provide no direct revenue or customer service benefit. Without this provision, the

algorithm could get stuck at a switched segment with capacitors but no customer load – closing that switch increases the losses but not the load served. Once the capacitors are switched on, the DEWorkstation load flow will operate their controls at each step. Another modification to (3.1) is that any switching operation with no loss increment has a merit figure of 0, even if the denominator is also 0. This lets the algorithm switch on zero-impedance branches that don't serve any direct load.

The algorithm stops when no suitable candidate can be closed in a given step. This may occur when:

1. all load has been served – there are no more candidates

2. no more switches can be closed without violating voltage or current constraints

Whenever a component's voltage or current constraint prevents an "attractive" candidate switch closing, the warning message on that component serves as a clue that the system might be upgraded in that area. The user can also modify the voltage and current constraint criteria to reflect emergency conditions.

3.5 Reconfiguration with Approximate Loss Screening

The algorithm in Figure 3.3 calls for a full nonlinear load flow to evaluate each candidate switching operation. This load flow runs on just one circuit, which will usually be a small subset of the total system. Figure 3.4 modifies the algorithm's main loop to use an approximate loss screening of each candidate, using (3.2) for the loss in each switched branch. The switched segment voltage is assumed constant and equal to the existing voltage behind the candidate switch, and the load current angles are assumed balanced. The voltage and current constraints are checked approximately, neglecting any decrease in the voltage at the switch. After selecting a best candidate this way, the algorithm runs a full nonlinear load flow and checks the constraints again. If this check fails, the algorithm repeats the step and all future evaluations of that candidate will use a full load flow. At the conclusion of each step in Figure 3.4, the algorithm always has a full load flow solution that satisfies all constraints, but the total number of load flows run is greatly reduced.

$$\begin{aligned} P_{loss} &= I_1^2 R_{11} + I_2^2 R_{22} + I_3^2 R_{33} \\ &\quad + 2R_{12}(A'_{re}B'_{re} + A'_{im}B'_{im}) + 2R_{13}(A'_{re}C'_{re} + A'_{im}C'_{im}) + 2R_{23}(B'_{re}C'_{re} + B'_{im}C'_{im}) \end{aligned} \tag{3.2}$$

$$I_1 = \sqrt{A_{re}^2 + A_{im}^2} \tag{3.3}$$

$$I_2 = \sqrt{B_{re}^2 + B_{im}^2} \tag{3.4}$$

$$I_3 = \sqrt{C_{re}^2 + C_{im}^2} \tag{3.5}$$

$$A_{re} = kWflow_1/kV_1 \tag{3.6}$$

$$A_{im} = kVARflow_1/kV_1 \tag{3.7}$$

$$B_{re} = kWflow_2/kV_2 \tag{3.8}$$

$$B_{im} = kVARflow_2/kV_2 \tag{3.9}$$

$$C_{re} = kWflow_3/kV_3 \tag{3.10}$$

$$C_{im} = kVARflow_3/kV_3 \tag{3.11}$$

$$A'_{re} = A_{re} \tag{3.12}$$

$$A'_{im} = A_{im} \tag{3.13}$$

$$B'_{re} = -0.5B_{re} + 0.866B_{im} \tag{3.14}$$

$$B'_{re} = -0.5B_{im} - 0.866B_{re} \tag{3.15}$$

$$C'_{re} = -0.5C_{re} - 0.866C_{im} \tag{3.16}$$

$$C'_{re} = -0.5C_{im} + 0.866C_{re} \tag{3.17}$$

In (3.2)-(3.11), the subscripts 1, 2, and 3 refer to three phase conductors, *R* refers to resistive elements of the branch series impedance matrix, *kWflow* is the nominal real power flow through the branch, *kVARflow* is the nominal reactive power flow through the branch, and *kV* is the voltage behind the candidate switch. Subscripts *re* and *im* refer to real and imaginary parts of the current, and primed quantities have been rotated to the same phase angle reference.

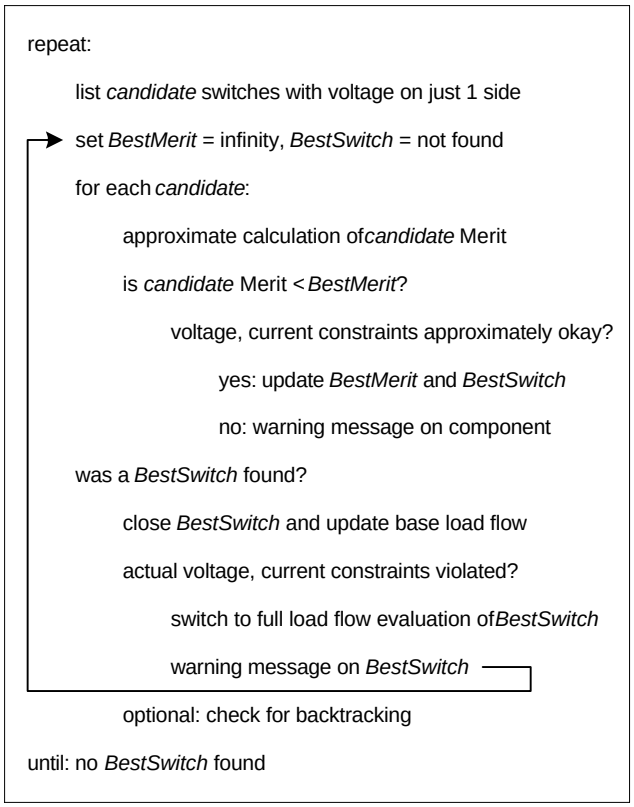

Figure 3.4 - Reconfiguration algorithm with approximate loss evaluation

3.6 Backtracking

Figures 3.3 and 3.4 show an optional backtracking step at the end of the main loop, further detailed in Figure 3.5. Whenever a switch closes to complete an open loop, at least one of the other candidates from that step will now have voltage on both sides. Those alternates are saved in a list structure, keyed on the switch that was actually selected to close. Subsequent steps in the algorithm may add load to that circuit, and make one of the alternates more attractive. The algorithm checks alternate feeds whenever a selected candidate switch has one or more of the open loop key switches in its feeder path. After opening the key switch, if an alternate feed has a higher voltage magnitude than the key switch, the algorithm runs a load flow to see if the losses decrease. If so, the key switch and best alternate are exchanged. An open loop may swap only once per step, but may swap again in a later step.

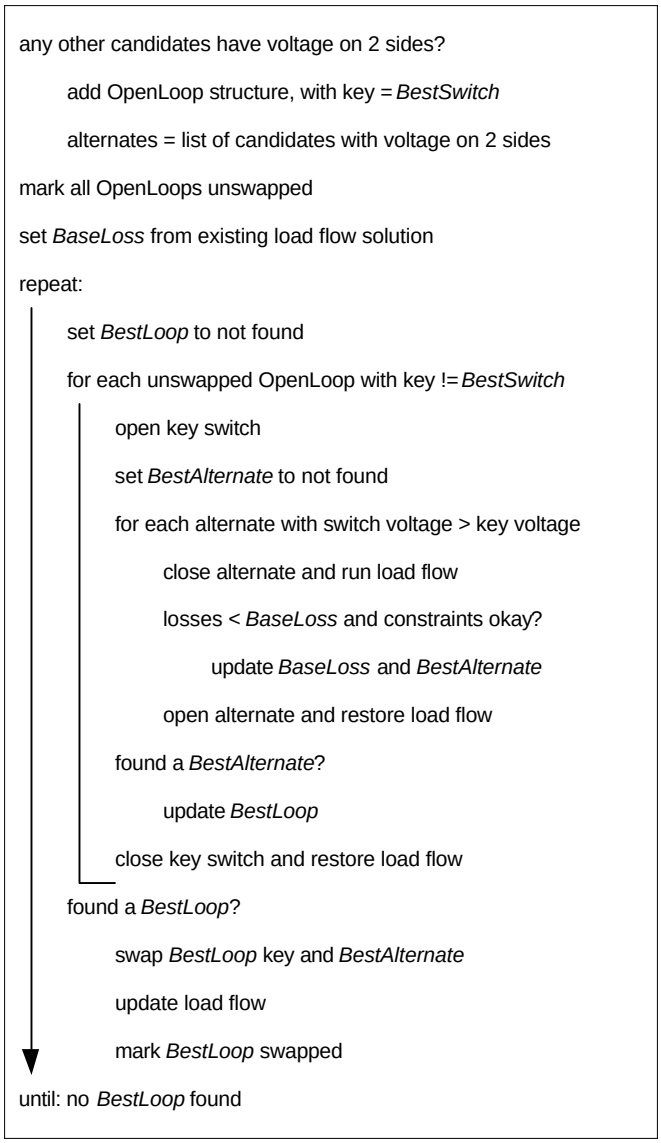

Figure 3.5 - Open loop backtracking scheme

3.7 Example Reconfiguration with Backtracking

Figure 3.6 shows a sample circuit from [Dolloff], used to illustrate how the basic algorithm works with backtracking. The series branches have been simplified to resistances, and the loads are modeled as constant current. The system voltage is 13.8 kV, but in this case (3.1) is modified to normalize by load current rather than load kVA. SWA is a proposed new switch location, not considered in the first algorithm solution. The base case has switches 3 and 5 open, with losses of 90.14 kW per phase. A network load flow with all switches closed produces losses of 66.36 kW per phase. Table 3.1 shows the switches closed, candidate switches, merit figures for each candidate, and best candidate at each step.

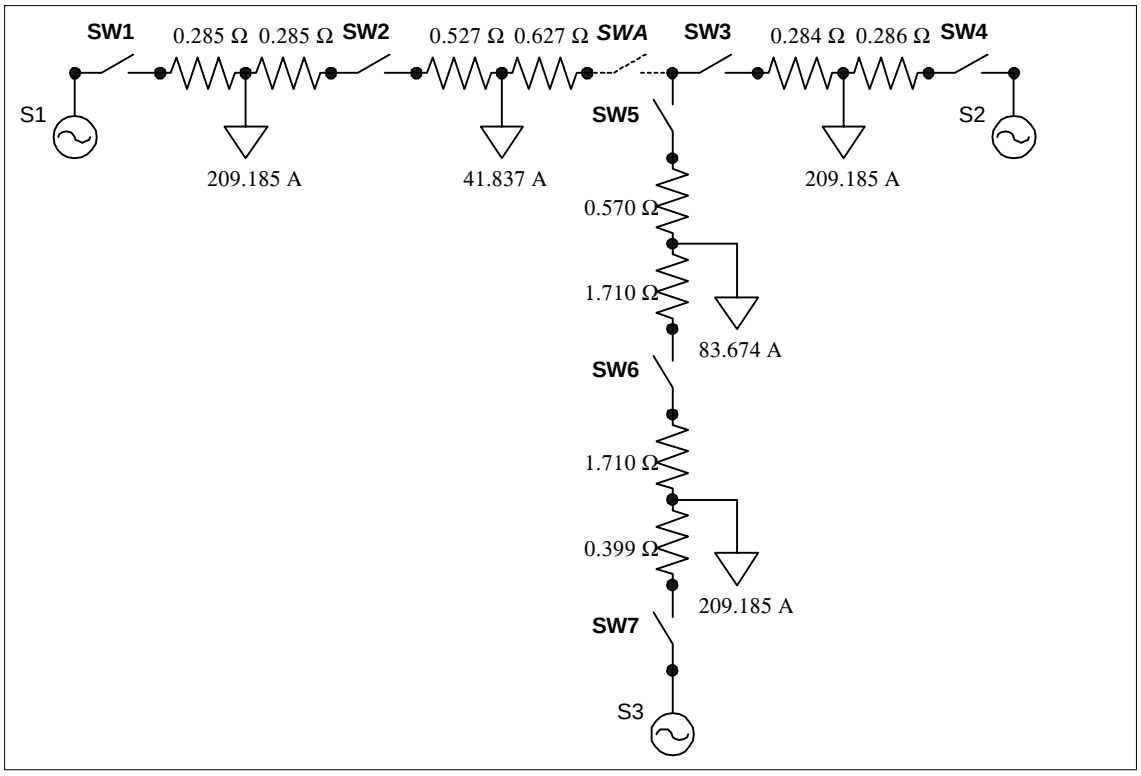

Figure 3.6 - Sample circuit with constant-current loads

Table 3.1 Reconfiguration algorithm steps for Figure 3.6

Step	Switches Closed	Candidates	Merit Figures	Best
1	none	1, 4, 7	59.62, 59.83, 83.46	1
2	1	2, 4, 7	165.13, 59.83, 83.46	4
3	1, 4	2, 3, 7	165.13, 169.73, 83.46	7
4	1, 4, 7	2, 3, 6	165.13, 169.73, 486.48	2
5	1, 2, 4, 7	5, 6	402.97, 486.48	5

To work through the solution step by step, the incremental load served by each candidate switch is taken from the load currents shown on Figure 3.6. The incremental loss is calculated by summing the I^2R loss in each resistance along the feeder path containing the candidate switch, then subtracting the previous total loss along that feeder path. The merit figure is the incremental loss divided by the incremental load.

DAOP Step 1 - no switches closed

The candidate switches in step 1 are SW1, SW4, and SW7. The calculation of each candidate's merit figure follows:

SW1: *Loss = 0.285 * 209.185 * 209.185 = 12471.13*

Load = 209.185

Merit = 12471.13 / 209.185 = 59.62

SW4: *Loss = 0.286 * 209.185 * 209.185 = 12514.89*

Load = 209.185

Merit = 12514.89 / 209.185 = 59.83

SW7: *Loss = 0.399 * 209.185 * 209.185 = 17459.59*

Load = 209.185

Merit = 17459.59 / 209.185 = 83.46

SW1 is closed because it has the lowest merit figure. Three feeder path load flow calculations were performed in this step.

DAOP Step 2 - SW1 already closed

The candidate switches in step 2 are SW2, SW4, and SW7.

SW2: *Loss = 0.285 * (209.185 + 41.837)^2 + (0.285 + 0.527) * 41.837^2 - 12471.13*

= 19379.70 - 12471.13 = 6908.57

Load = 41.837

Merit = 165.13

SW4: *Merit = 59.83 from step 1*

SW7: *Merit = 83.46 from step 1*

SW4 is closed because it has the lowest merit figure. One feeder path load flow calculation was performed in this step, for SW2. We did not have to repeat the load flow calculations for SW4 and SW7.

DAOP Step 3 - SW1 and SW4 already closed

The candidate switches in step 3 are SW2, SW3, and SW7.

SW2: *Merit = 165.13 from step 2*

SW3: *Loss = 0.286 * (209.185 + 41.837)^2 + (0.284 + 0.627) * 41.837^2 - 12514.89*

= 19616.00 - 12514.89 = 7101.11

Load = 41.837

Merit = 7101.11 / 41.837 = 169.73

SW7: *Merit = 83.46 from step 1*

SW7 is closed because it has the lowest merit figure. One feeder path load flow calculation was performed in this step.

DAOP Step 4 - SW1, SW4, and SW7 already closed

The candidate switches in step 4 are SW2, SW3, and SW6.

SW2: *Merit = 165.13 from step 3*

SW3: *Merit = 169.73 from step 3*

SW6: *Loss* $= 0.399 * (209.185 + 83.674)^2 + (1.71 + 1.71) * 83.674^2 - 17459.59$

$= 58165.37 - 17459.59 = 40705.78$

Load = 83.674

Merit = 40705.78 / 83.674 = 486.48

SW2 is closed because it has the lowest merit figure. This operation causes SW3 to have power supplied on both sides, so SW3 cannot be closed in any subsequent step. For possible backtracking, we will remember that SW2 is an open loop key switch, and that SW3 is its corresponding open loop alternate switch.

One feeder path load flow calculation was performed in this step.

DAOP Step 5 - SW1, SW2, SW4, and SW7 already closed

The candidate switches in step 5 are SW5 and SW6.

SW5: *Loss* $= 0.285 * (209.185 + 41.837 + 83.674)^2$

$+ (0.285 + 0.527) * (41.837 + 83.674)^2$

$+ (0.627 + 0.570) * 83.674^2 - 19379.70$

$= 53098.15 - 19379.70 = 33718.45$

Load = 83.674

Merit = 33718.45 / 83.674 = 402.97

SW6: *Merit = 486.48 from step 4*

SW5 is closed because it has the lowest merit figure. One feeder path load flow calculation was performed in this step. There have been a total of seven feeder path load flow calculations during the solution so far; but none of these have needed to solve the whole system.

DAOP Backtracking at Step 5

The solution after step 5 has SW3 and SW6 open, with losses of 83.75 kW per phase. When the algorithm finishes, the sequence of partial load flows has constructed a full system load flow solution, and the total system loss will be available without a repeat load flow solution.

When SW5 is closed at step 5, the open loop key switch SW2 is found in SW5's new feeder path. Exchanging the key switch SW2 with its alternate SW3, which had been identified in step 4, the system losses decrease from 83.75 kW per phase to 71.53 kW per phase. Thus, the simple backtracking procedure in Figure 3.5 improves the solution for this example, and in many of the other test cases examined.

Referring to Figure 3.6, note that SW2 is electrically closer to the 41.837-ampere load than SW3 is. This is why SW2 is preferred at step 4. In the next step, a larger 83.674-ampere load must be served, and SW3 is electrically closer to this larger load than is SW2. The alternative SW6 is not attractive. The DAOP algorithm has been "fooled" by the 41.837-ampere load, and commits to SW2 too early. The single-step backtracking scheme helps to mitigate this greedy nature of DAOP.

The entire solution with backtracking has required seven partial load flows for candidate switch evaluation, plus another load flow on two feeder paths for the backtracking step.

Transshipment Solution

The problem in Figure 3.6 can also be solved using the linearized transshipment method described in section 2.4. Assuming all line segments have the same current capacity, the segment cost will be the sum of resistances between the candidate switch and the load it serves. The transshipment algorithm starts with all switches open.

Transshipment Step 1 - no switches closed

The candidates in step 1 are SW1, SW4, and SW7. The segment costs are:

SW1: *Cost = 0.285*

SW4: *Cost = 0.286*

SW7: *Cost = 0.399*

SW1 has the lowest cost, so its 209.185-ampere load will be picked up first. There are no other switches that can serve this load, so SW1 is closed. No load flow calculations were performed in this step.

Transshipment Step 2 - SW1 already closed

The candidates in step 2 are SW2, SW4, and SW7. The segment costs are:

SW2: *Cost = 0.285 + 0.527 = 0.812*

SW4: *Cost = 0.286*

SW7: *Cost = 0.399*

SW4 has the lowest cost, and no other switch can serve its 209.185-ampere load. SW4 is closed.

Transshipment Step 3 - SW1 and SW4 already closed

The candidates in step 3 are SW2, SW3, and SW7. The segment costs are:

SW2: *Cost = 0.285 + 0.527 = 0.812*

SW3: *Cost = 0.284 + 0.627 = 0.911*

SW7: *Cost = 0.399*

SW7 has the lowest cost, and no other switch can serve its 209.185-ampere load. SW7 is closed.

Transshipment Step 4 - SW1, SW4, and SW7 already closed

The candidates in step 4 are SW2, SW3, and SW6. The segment costs are:

SW2: *Cost = 0.285 + 0.527 = 0.812*

SW3: *Cost = 0.284 + 0.627 = 0.911*

SW6: *Cost = 1.71 + 1.71 = 3.42*

SW2 has the lowest cost, so the 41.837-ampere load will be picked up next. SW3 can also serve this load, so the transshipment algorithm will check both SW2 and SW3, and close the one that results in the lowest losses. Glamocanin used an approximate loss formulation to do this, but a full load flow solution could also be done. Using either method, closing SW2 will result in the lowest losses, and the algorithm will select SW2. It is the 83.674-ampere load that changes this selection; since it has not been served yet, the transshipment algorithm does not account for it.

Transshipment Step 5 - SW1, SW2, SW4, and SW7 already closed

The candidates in step 5 are SW5 and SW6. The segment costs are:

SW5: *Cost = 0.627 + 0.57 = 1.197*

SW6: *Cost = 1.71 + 1.71 = 3.42*

SW5 has the lowest cost, so the 83.674-ampere load will be picked up next. SW6 can also serve this load, but it will be found to produce greater losses than SW5. Therefore, SW5 is closed and

the transshipment algorithm solution is complete. At this point, a full system load flow will calculate the total losses as 83.75 kW per phase.

Comparison of DAOP and Transshipment Algorithms

The transshipment solution is the same as the DAOP solution without backtracking. The transshipment algorithm in practice would require one feeder path load flow at the end of each step to verify the voltage and current constraints, plus two more feeder path load flows in steps 4 and 5, to evaluate the alternate switches SW3 and SW6. This is approximately the same computational burden as DAOP with no backtracking. The DAOP algorithm can account for nonlinearities and control action during the candidate switch evaluations, which is an advantage.

With backtracking, DAOP requires more load flow calculations than transshipment, but it reaches a better solution. This is also an advantage over the linearized algorithm. Use of the full load flow calculation would not help the transshipment solution in this case. Adding a switch exchange algorithm at the end of the transshipment solution might be helpful in this case. However, Glamocanin stated that a prime motivation for the transshipment algorithm was to avoid switch exchanges.

Chapter 4

Test Cases

Tables 4.1 through 4.3 summarize results for a variety of test systems used in the literature. A constant-current load model was used for all results in Table 4.2, except for the Baran and Wu circuit, which used a constant-power load model. Since the algorithm runs load flows on one circuit at a time, a rough measure of system size would be the number of switches divided by the number of circuits. By this measure, the Baran and Wu system is much larger than the others. The algorithm, run with backtracking and approximate loss screening, reached the best solution in all these cases, including the improved solution reported in [Goswami] for the Baran and Wu system. The algorithm worked with either constant-current or constant-power loads in all test systems, and with various capacitor configurations in the two systems that have capacitors.

Each system was tested with a variety of component failures, and the algorithm served as much load as possible while minimizing losses. In those cases, the losses decrease compared to the unfaulted state reported in Table 4.2.

The running time is mostly dependent on the number of full load flows run, and Table 4.3 shows about a six-to-one reduction in load flows by using the approximate loss evaluation. In all tests examined so far, the approximate loss evaluation produces the same reconfiguration as the full load flow screening.

Table 4.1 Test System Size Characteristics

Test System	Circuits	Loads	Lines	Switches	Capacitors
Dolloff	3	5	10	8	0
Civanlar 2-Feeder	2	10	11	12	0
Civanlar 3-Feeder	3	13	16	17	7
Glamocanin	3	9	13	13	0
Baldick Discussion	1	2	4	5	1
Baran and Wu	1	32	37	37	0

Table 4.2 Benchmark, networked, and final system losses [kW]

Test System	Benchmark	Network	Final
Dolloff	270.41	199.08	202.28
Civanlar 2-Feeder	310.00	305.22	306.04
Civanlar 3-Feeder	488.46	412.34	447.45
Glamocanin	255.65	229.53	247.49
Baldick Discussion	18.78	10.63	15.75
Baran and Wu	202.68	124.55	142.60

Table 4.3 Simulation times on a Pentium 90 [seconds]

Test System	Network	Full	Approximate
Dolloff	1.867	2.910	0.988
Civanlar 2-Feeder	1.373	5.384	1.153
Civanlar 3-Feeder	3.625	15.658	2.964
Glamocanin	2.966	6.373	0.933
Baldick Discussion	0.494	1.373	0.220
Baran and Wu	14.063	226.697	20.451

In DEWorkstation, the test circuits are modeled by drawing the line segments, switches, substations, and capacitor banks. The branch impedances are entered through editing dialogs for each line segment. For other components, including substations, capacitor banks, and line voltage regulators, the user must enter the equipment data into DEWorkstation's parts library, before placing these parts on the schematic. Sections 4.1 through 4.7 list all of the required parts, branch impedance, and load data needed to model the test circuits in DEWorkstation.

Most of the published examples list bus loads, which is the normal practice for networked transmission and subtransmission systems. DEWorkstation associates loads with line segments, which is common practice for radial distribution systems. The DEWorkstation assumes all segment load is lumped at the far end of the line segment, to give conservative estimates of the voltage drop. If a segment is switched to an alternate feed, its load can move from one end to the other in DEWorkstation's model. In order to make valid comparisons, the load locations must be the same as in the published results. In DEWorkstation, this was accomplished using zero-impedance stubs at each bus, with all load at that bus represented as a spot load on that stub segment.

4.1 Dolloff's Circuit

The system shown in Figure 3.6 was modeled in DEWorkstation to verify the algorithm's computer implementation. At a nominal substation voltage of 13.8 kV line-to-line, the constant-current loads in Figure 3.6 are input as the kW loads specified in Table 4.4. The branch impedances are specified with the resistance values given in Figure 3.6, and a transformer turns ratio of 63.5:1 in each line segment. At 13.8 kV, this transformer turns ratio produces a customer service voltage of 120 volts:

$$13800/(\sqrt{3} * 63.51) = 120.0 \qquad (4.1)$$

Table 4.4 Load data for Dolloff's circuit in DEWorkstation

Current [A]	Power [kW]
41.837	1000.0
83.674	2000.0
209.185	5000.0

The DEWorkstation solutions of Dolloff's circuit use three-phase losses, which are three times the per-phase values calculated in section 3.7. In the base case with SW3 and SW5 open, which looks symmetrical on Figure 3.6, the total losses are 270.41 kW. Running the algorithm without backtracking produces a configuration of SW3 and SW6 open, with total losses of 251.25 kW. Repeating the solution with backtracking, the algorithm finds the correct solution of SW2 and SW6 open, with total losses of 214.59 kW. The network system losses are 190.07 kW, so most of the available improvement has been achieved with SW2 and SW6 open.

The use of backtracking indicates a possible benefit from installing more switches in that area. If SWA is installed, the optimal solution has SWA and SW6 open, with losses of 202.27 kW. Compared to the network solution, very little improvement is possible.

4.2 Civanlar 2-Feeder Circuit

Table 4.5 contains the branch impedance and bus load data for Civanlar's 2-Feeder test circuit. The nominal substation voltage is 23 kV line-to-line, which requires a distribution transformer turns ration of 110.0:1 in each line segment. There are no current constraints given.

Table 4.5 Impedance and load data for Civanlar 2-Feeder circuit

Bus		Impedance [ohms]		Load at To Bus [kVA]	
From	**To**	**R**	**X**	**P**	**Q**
A	5	0.3968	0.5290	2000.0	600.0
5	4	0.4232	0.5819	3000.0	1300.0
4	3	0.4761	0.6348	2000.0	500.0
3	2	0.2116	0.2116	1500.0	300.0
2	1	0.1587	0.1587	500.0	100.0
1	1'	0.2116	0.0529	1000.0	200.0
1'	2'	0.5290	0.5290	1500.0	200.0
2'	3'	0.5819	0.5819	2500.0	600.0
3'	4'	0.4761	0.6348	3000.0	400.0
4'	5'	0.2910	0.5819	2500.0	900.0
5'	B	0.5290	0.5290		

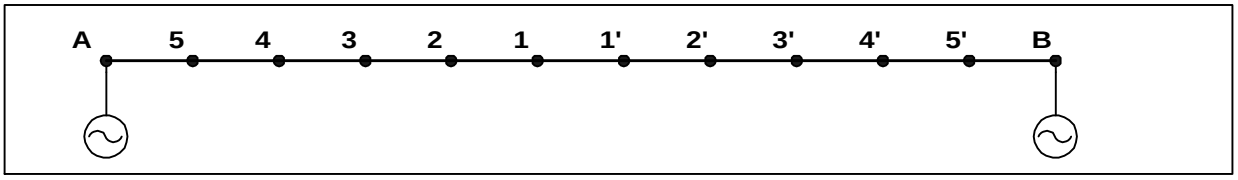

Figure 4.1 - Civanlar's 2-Feeder Test Circuit

Civanlar's 2-feeder test circuit does not require backtracking. The algorithm was tested with both constant current and constant power load models, and reached the same configuration (1'-2' open) in both cases.

4.3 Civanlar 3-Feeder Circuit

Table 4.6 contains the branch impedance and bus load data for the circuit in Figure 4.2. The nominal substation voltage is 23 kV line-to-line, which requires a distribution transformer turns ratio of 110.0:1 in each line segment. The capacitor banks are all wye grounded, and comprised of parallel combinations of units rated 300 kVAR and 100 kVAR at 23 kV.

Figure 4.2 shows the base case, and Figure 4.3 shows the optimal configuration found by the DAOP algorithm. The solution in Figure 4.3 matches that found by Civanlar. This test case illustrates that the DAOP algorithm works with capacitor banks. No voltage or current constraints were encountered, but backtracking was initiated during the solution.

Table 4.6 Impedance and load data for Civanlar 3-Feeder circuit

Bus		Impedance [ohms]		Load at To Bus [kVA]		
From	**To**	**R**	**X**	**P**	**Q**	**Cap Bank**
1	4	0.3968	0.5290	2000.0	1600.0	
4	5	0.4232	0.5819	3000.0	1500.0	1100.0
4	6	0.4761	0.9522	2000.0	800.0	1200.0
6	7	0.2116	0.2116	1500.0	1200.0	
2	8	0.5819	0.5819	4000.0	2700.0	
8	9	0.4232	0.5819	5000.0	3000.0	1200.0
8	10	0.5819	0.5819	1000.0	900.0	
9	11	0.5819	0.5819	600.0	100.0	600.0
9	12	0.4232	0.5819	4500.0	2000.0	3700.0
3	13	0.5819	0.5819	1000.0	900.0	
13	14	0.4761	0.6348	1000.0	700.0	1800.0
13	15	0.2432	0.5819	1000.0	900.0	
15	16	0.2116	0.2116	2100.0	1000.0	1800.0
5	11	0.2116	0.2116			
10	14	0.2116	0.2116			
7	16	0.4761	0.6348			

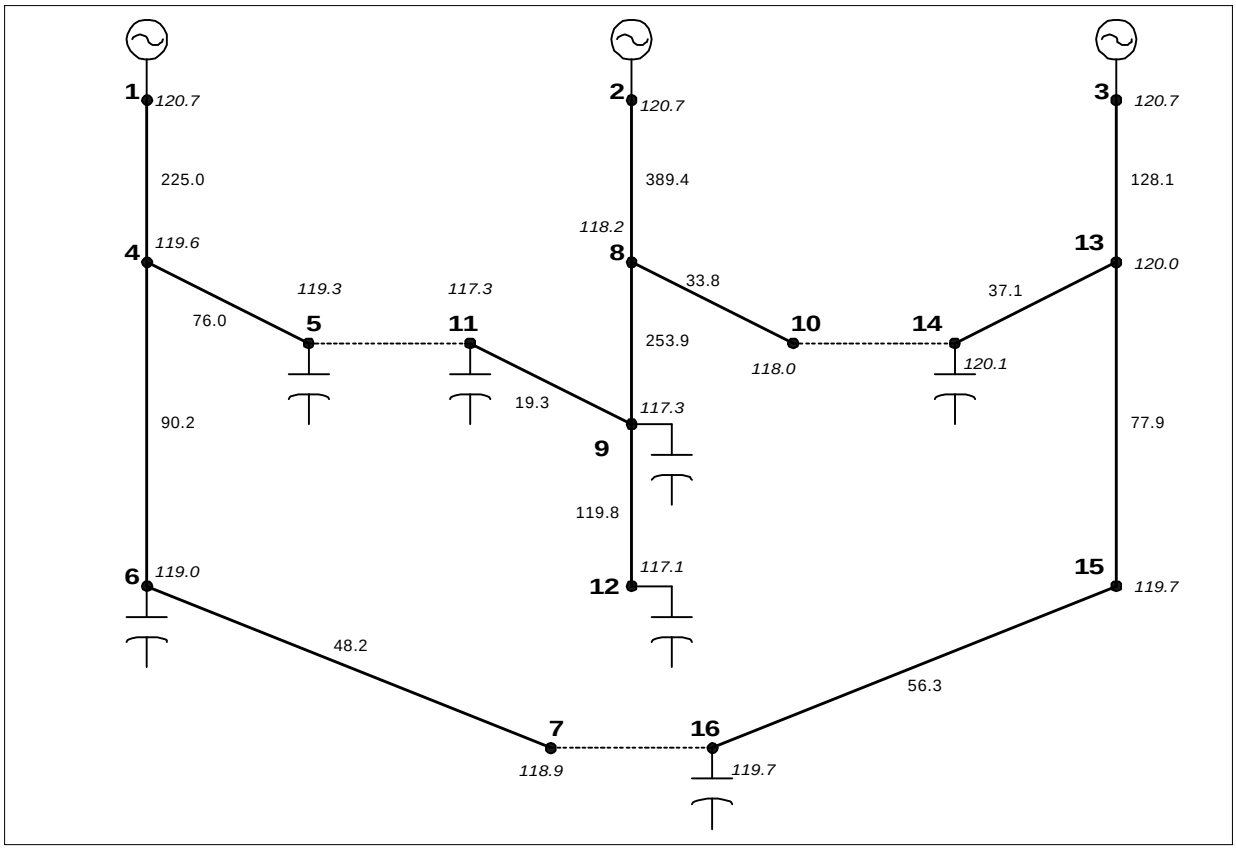

Figure 4.2 - Civanlar's 3-Feeder Test Circuit before Reconfiguration (line flows are in amperes, customer service voltage is *italicized*)

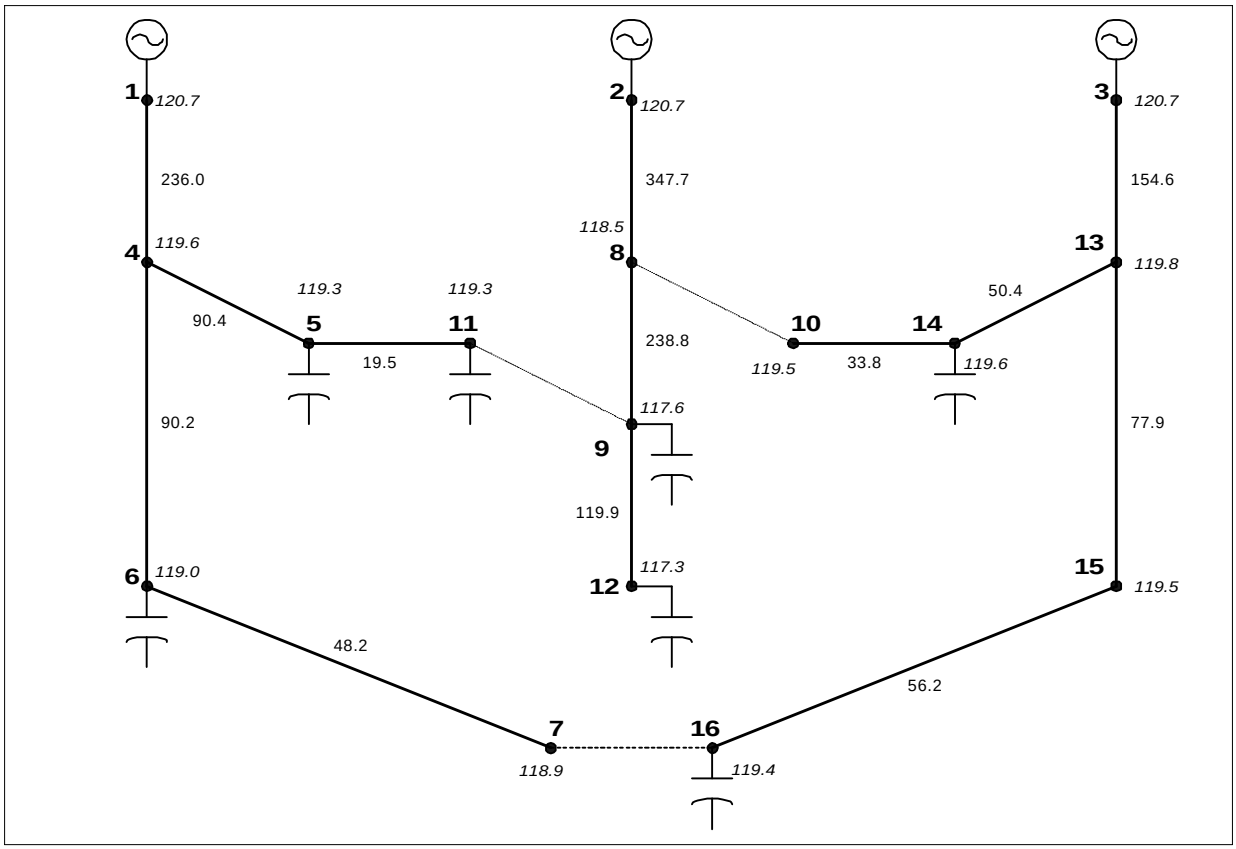

Figure 4.3 - Civanlar's 3-Feeder Test Circuit after Reconfiguration (line flows are in amperes, customer service voltage is *italicized*)

4.4 Glamocanin Circuit

Table 4.7 contains the branch impedance and bus load data for the circuit shown in Figure 4.4. In DEWorkstation, the impedances are entered directly from Table 4.7, but each line segment is assigned a conductor with a rating of 194 amperes. This conductor assignment matches the current constraint used in [Glamocanin]. The nominal substation voltage is 10 kV line-to-line, because the example is based on a European system. The distribution transformer ratio is 48.11:1 in each line segment. The voltage drop constraint is 5%, corresponding to a customer service voltage of 114 volts.

Figure 4.4 shows the base case load flow solution, and Figure 4.5 shows the load flow solution after the DAOP algorithm's reconfiguration. Figure 4.5 matches the configuration found by Glamocanin. Voltage constraints were encountered and successfully handled during the solution. Glamocanin pointed out that the branch exchange method would not work on the base case shown in Figure 4.4, due to voltage and current constraints.

Table 4.7 Impedance and load data for Glamocanin circuit

Bus		Impedance [ohms]		Load at To Bus [kVA]	
From	**To**	**R**	**X**	**P**	**Q**
1	2	0.7820	0.2120	600.0	400.0
1	3	0.7820	0.2120	500.0	300.0
1	4	1.5640	0.4240	100.0	90.0
2	5	0.7820	0.2120	600.0	400.0
2	6	1.1730	0.3180	1300.0	1100.0
3	7	1.3685	0.3710	1300.0	1000.0
4	8	1.1730	0.3180	100.0	90.0
3	9	0.7820	0.2120	800.0	600.0
2	10	1.1730	0.3180	300.0	100.0
3	5	1.1730	0.3180		
6	9	0.7820	0.2120		
8	9	1.1730	0.3180		
4	10	1.1730	0.3180		

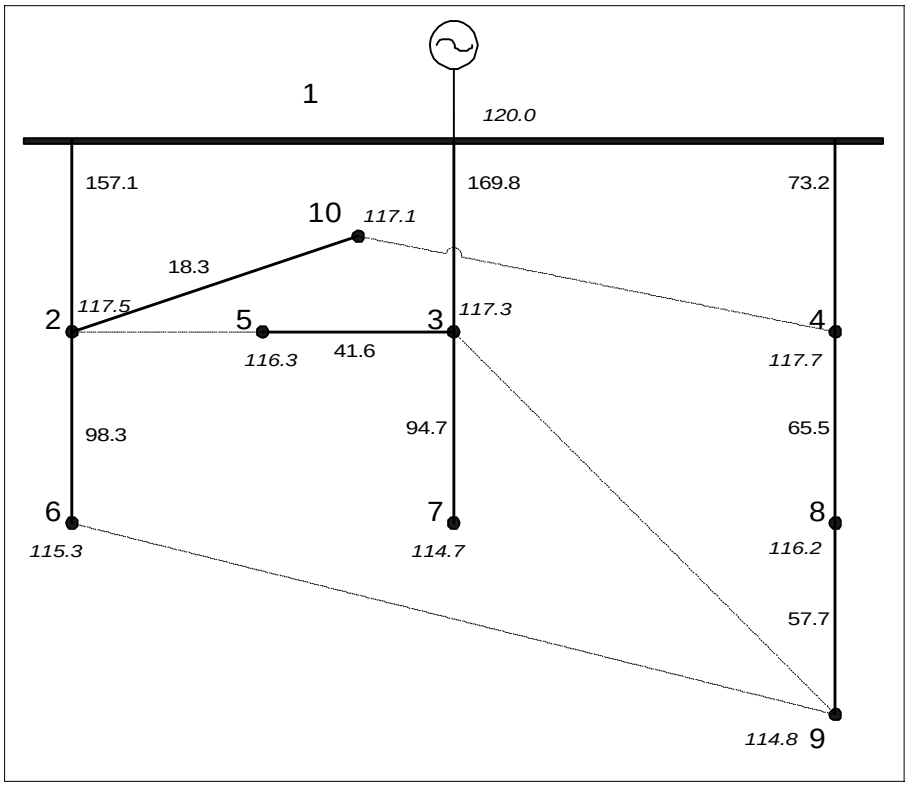

Figure 4.4 - Glamocanin's Test Circuit before Reconfiguration (line flows are in amperes, customer service voltage is *italicized*)

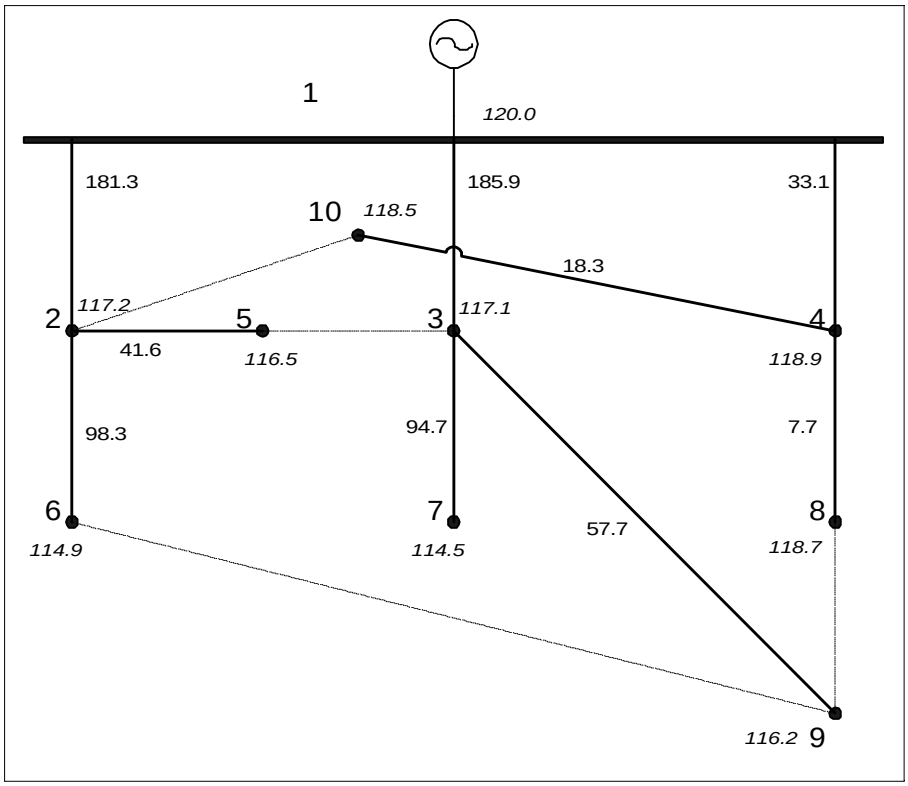

Figure 4.5 - Glamocanin's Test Circuit after Reconfiguration (line flows are in amperes, customer service voltage is *italicized*)

4.5 Baldick Discussion Circuit

Figure 4.6 shows the test circuit with a capacitor bank from Baldick's discussion of [Glamocanin]. The nominal substation voltage is 13.8 kV line-to-line, which requires a distribution transformer turns ratio of 63.5:1 in each segment. The 50-ampere load is 1195 kW three-phase at 13.8 kV, and the 100+j100 ampere load is 2390 kW plus 2390 kVAR at 13.8 kV. The 100-ampere capacitor bank was modeled with a 1951.706 kVAR bank at 12.47 kV.

The pure transshipment algorithm does not find the optimal configuration for this circuit, as discussed in section 2.4. The DAOP algorithm works, because it assigns a low but non-zero weight to shunt capacitor banks in the merit figure. The weight is not zero, because in some configurations that can act as a barrier to the DAOP algorithm. With a capacitor bank weighting of zero, DAOP would never close a switch that served just a capacitor bank, because that would increase losses with no corresponding increase in load served. If there were customer loads beyond the capacitor bank, and no alternate feeds for those customer loads, they would never be served in the DAOP algorithm.

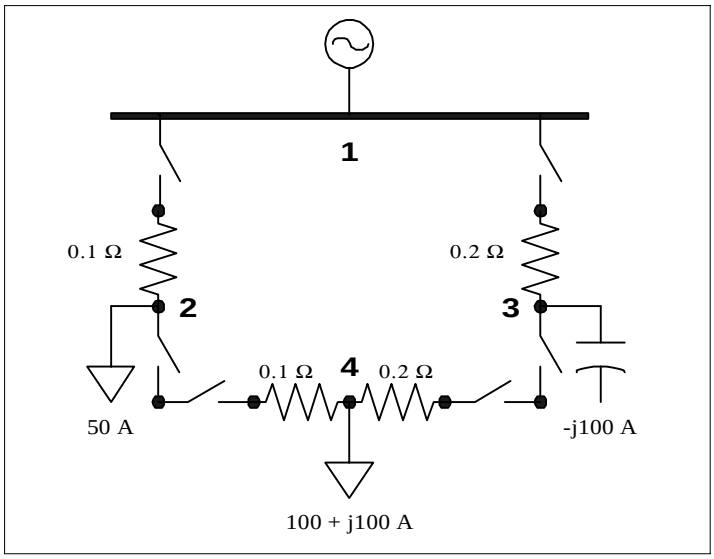

Figure 4.6 - Baldick's Discussion Test Circuit

4.6 Baran and Wu Circuit

Table 4.8 contains the branch impedance and bus load data for the circuit in Figure 4.7. The substation voltage is 12.66 kV line-to-line, which requires a transformer ratio of 60.91:1 in each segment.

This test circuit is more severe than the others, because of the low voltage conditions, the large reactive load at bus 29, and the number of tie switches within a single feeder. To solve this circuit with the DAOP algorithm, an emergency voltage limit of 110 volts must be specified, corresponding to the ANSI B range. Otherwise, the DAOP algorithm will stop before serving all the load, due to voltage constraints. The optimal configuration in Figure 4.8 has lower system losses, but still does not meet the normal operating voltage criteria of at least 114 volts.

The solution in Figure 4.8, which was obtained using backtracking, matches the one found by Goswami and Basu. The solution originally reported by Baran and Wu, obtained using their own algorithm and the loop cutting algorithm, was slightly less optimal than Figure 4.8, with approximately 600 watts additional loss. In practice, the difference would not be significant, and this illustrates why it is not always necessary to find the absolute global optimum.

In most cases, the merit figure can be calculated with the customer load's real power in the denominator. This has the advantage of corresponding directly to the utility's revenue-earning load. For the Baran and Wu test case, the merit figure was altered to use the customer load's apparent power. Otherwise, the large reactive load at bus 29 caused the DAOP algorithm to find a sub-optimal solution. The real and reactive loads at bus 29 must be served together, so they should be combined as apparent power in the merit figure. Considering only the real power, the losses increase by a disproportionate amount due to the current drawn by the reactive load, and this biases the DAOP solution in favor of other bus loads. Most loads have real power greater

than reactive power, so the difference is not important. After making this change in the merit figure, all test cases were repeated and produced the same results.

The other test cases described in this chapter involve at least two feeders. The test circuit in Figures 4.7 and 4.8 has just one source, representing a single feeder with parallel branches. Each load flow in DAOP amounts to a full system load flow in this test case, because there are no other circuits to exclude from the load flow solution. The DAOP algorithm would be relatively more efficient when there are multiple sources.

Table 4.8 Impedance and load data for Baran and Wu circuit

Bus		Impedance [ohms]		Load at To Bus [kVA]	
From	**To**	**R**	**X**	**P**	**Q**
0	1	0.0922	0.0470	100.0	60.0
1	2	0.4930	0.2511	90.0	40.0
2	3	0.3660	0.1864	120.0	80.0
3	4	0.3811	0.1941	60.0	30.0
4	5	0.8190	0.7070	60.0	20.0
5	6	0.1872	0.6188	200.0	100.0
6	7	0.7114	0.2351	200.0	100.0
7	8	1.0300	0.7400	60.0	20.0
8	9	1.0440	0.7400	60.0	20.0
9	10	0.1966	0.0650	45.0	30.0
10	11	0.3744	0.1238	60.0	35.0
11	12	1.4680	1.1550	60.0	35.0
12	13	0.5416	0.7129	120.0	80.0
13	14	0.5910	0.5260	60.0	10.0
14	15	0.7463	0.5450	60.0	20.0
15	16	1.2890	1.7210	60.0	20.0
16	17	0.7320	0.5740	90.0	40.0
1	18	0.1640	0.1565	90.0	40.0
18	19	1.5042	1.3554	90.0	40.0
19	20	0.4095	0.4784	90.0	40.0
20	21	0.7089	0.9373	90.0	40.0
2	22	0.4512	0.3083	90.0	50.0
22	23	0.8980	0.7091	420.0	200.0
23	24	0.8960	0.7011	420.0	200.0
5	25	0.2030	0.1034	60.0	25.0
25	26	0.2842	0.1447	60.0	25.0
26	27	1.0590	0.9337	60.0	20.0
27	28	0.8042	0.7006	120.0	70.0
28	29	0.5075	0.2585	200.0	600.0
29	30	0.9744	0.9630	150.0	70.0
30	31	0.3105	0.3619	210.0	100.0
31	32	0.3410	0.5302	60.0	40.0
7	20	2.0000	2.0000		
8	14	2.0000	2.0000		
11	21	2.0000	2.0000		
17	32	0.5000	0.5000		
24	28	0.5000	0.5000		

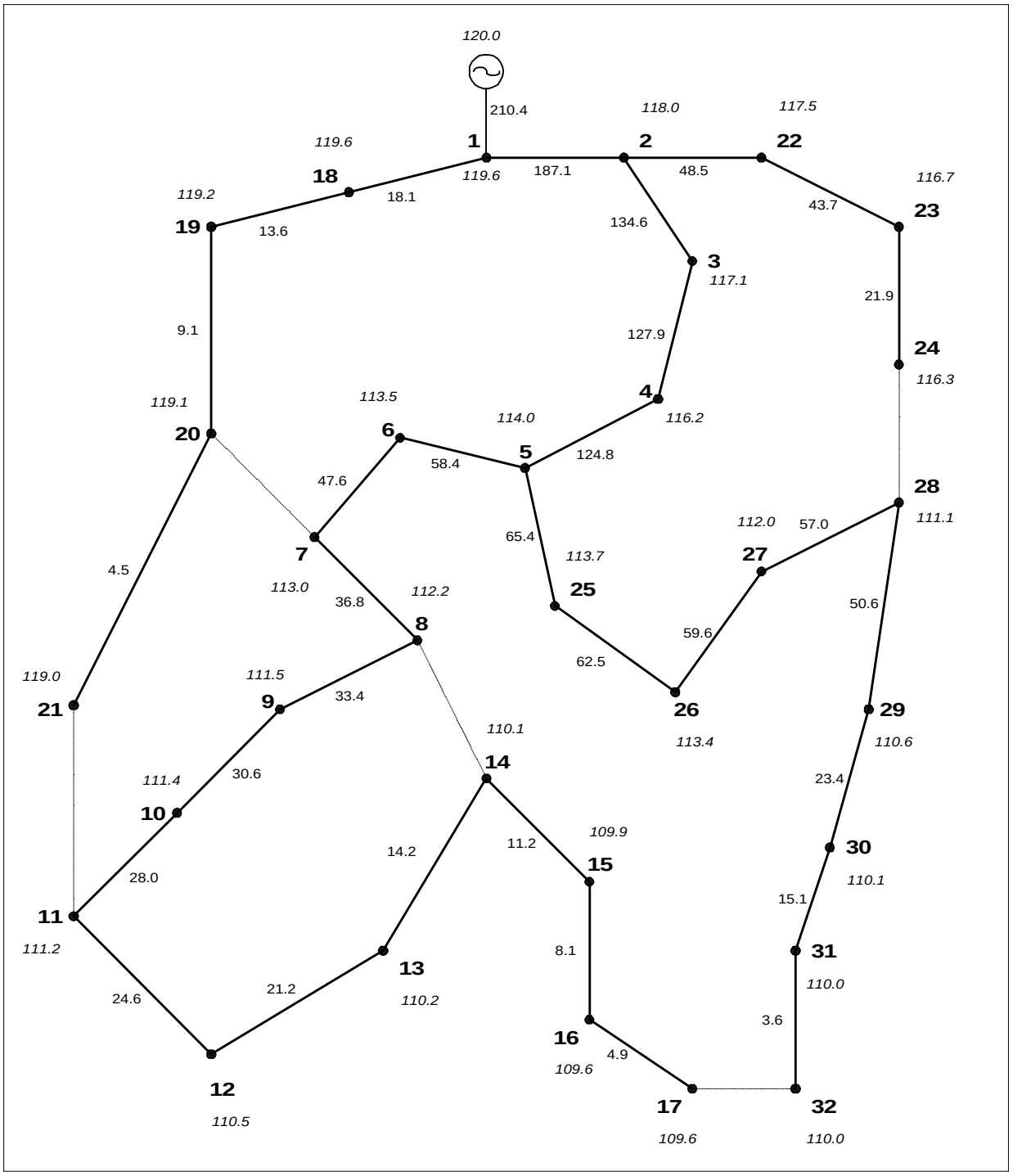

Figure 4.7 - Baran and Wu's Test Circuit Before Reconfiguration (line flows are in amperes, customer service voltage is *italicized*)

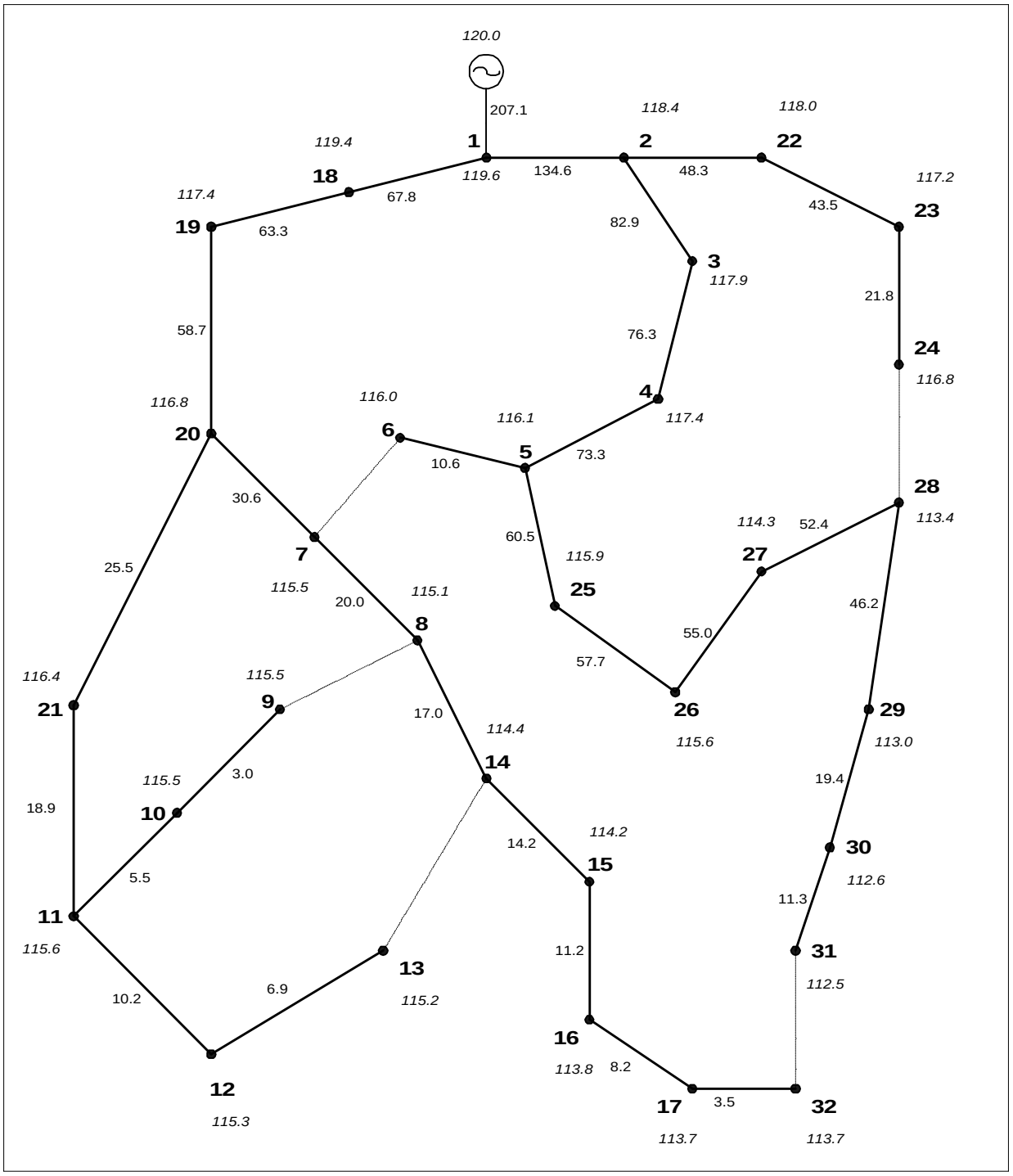

Figure 4.8 - Baran and Wu's Test Circuit After Reconfiguration (line flows are in amperes, customer service voltage is *italicized*)

4.7 Baran and Wu Circuit with Voltage Regulator

The Baran and Wu test system is shown in Figure 4.9, with two line voltage regulators added. Each line regulator is rated 12.66 kV line-to-line and 10 MVA, for a continuous current rating of 1400 amperes. The leakage impedance is 0.5 ohms, the winding losses are 1 watt, and the magnetizing current is 1 ampere. Each regulator is set for 120 volts, with a deadband of 2 volts, and no line drop compensation.

In the base case, with the 5 segments shown in dashed lines open, the service voltage is 109.6 volts at bus 17. This would violate an emergency limit of 110 volts. After the optimal reconfiguration of four switch exchanges shown in Figure 4.9, the service voltage is still 112.5 volts at bus 31. This would violate a normal limit of 114 volts. The utility might use line voltage regulators to deal with these voltage problems, as shown in Figure 4.9. Note that after the optimal switch swaps, the two regulators are not in series. With these regulators, the base case losses are 196.91 kW with a minimum service voltage of 116.3 volts at bus 24. The reconfiguration algorithm finds the same optimal switch exchanges, with total losses of 137.32 kW and a minimum service voltage of 115.2 volts at bus 13. During the solution, the regulator controllers move the taps appropriately during each load flow. This example illustrates how the reconfiguration algorithm can simulate control action, although in practice, the circuit in Figure 4.9 should also have some shunt capacitor banks installed.

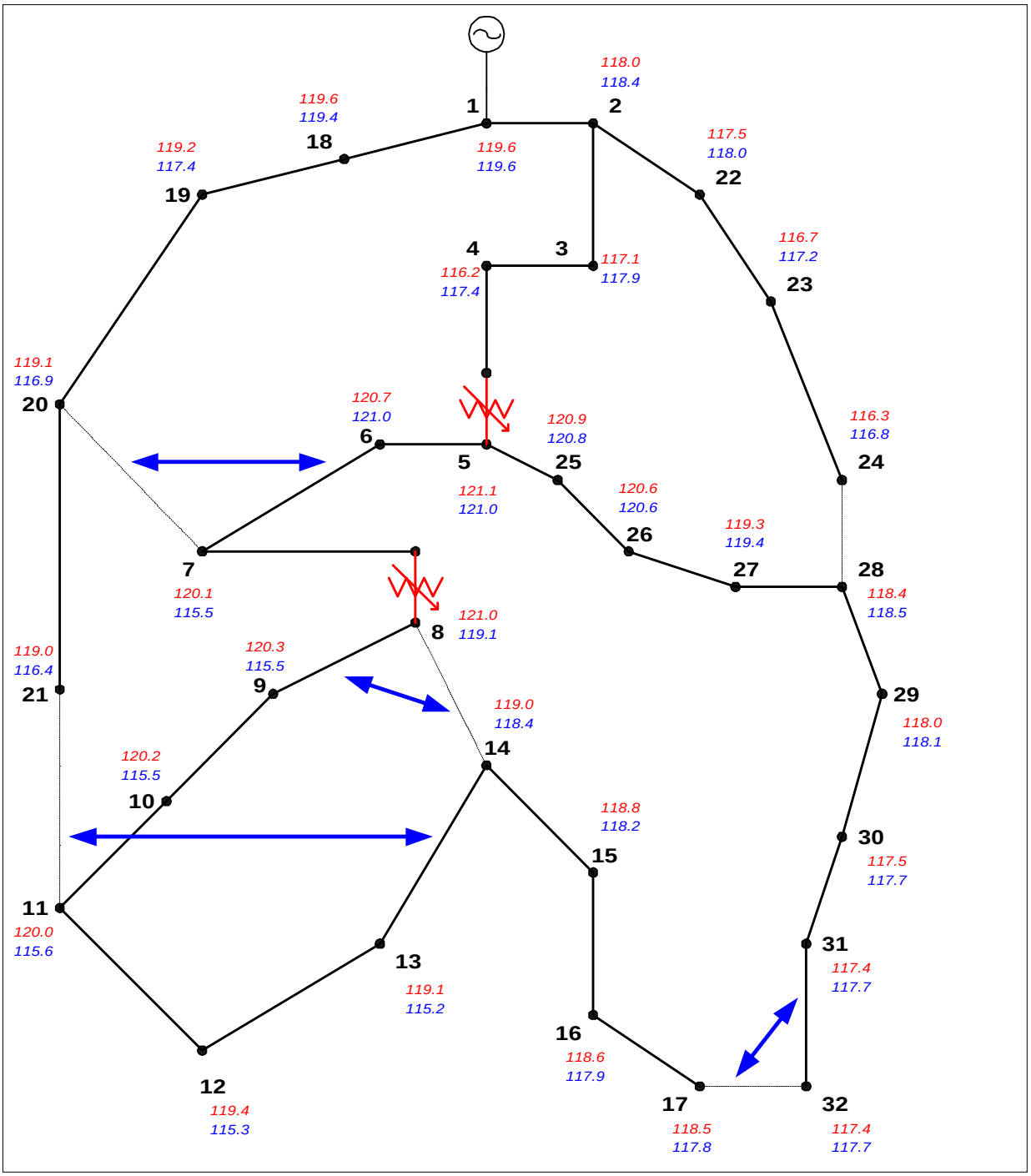

Figure 4.9 - Baran and Wu's Test Circuit with Voltage Regulators (customer service voltage before reconfiguartion in red, after reconfiguration in blue)

Chapter 5

Conclusions

This algorithm differs from most others, by constructing the system from scratch, rather than performing switch exchanges or sequential switch openings. An approximate loss formula helps to quickly screen candidate switch closings, but this method still performs more load flow calculations than other methods. Most of the load flow calculations only work with a subset of the system. The algorithm can solve either load restoration or loss minimization problems.

Several test cases show that this algorithm reaches the same optimal solutions found by other investigators. The execution time is longer, but constraints and control actions are handled more accurately. One of the test cases with line voltage regulators, described in Section 4.7, can not be solved properly with other published reconfiguration algorithms.

The work reported here builds on the linearized transshipment algorithm [Glamocanin] and discrete ascent optimal programming [Dolloff]. The original contributions of this work, not previously reported, are:

1. The reconfiguration algorithm considers control action and other nonlinear effects during the solution, not after the optimal configuration has been found. This affects both the loss evaluation and the feasible switching operations, as illustrated by the voltage regulator example in Section 4.7.

2. Approximate loss formulas were developed in Section 3.5 to screen candidate switching operations, making use of partial load flow solutions. After a candidate switch has been selected, the algorithm updates the complete load flow solution. In all test cases evaluated, screening with the approximate loss formulas produced the same solution as screening with full load flow solutions.

3. The heuristic backtracking method presented in Section 3.6 was developed to mitigate the greedy nature of DAOP, solving one of the problems encountered by Dolloff.

4. The DAOP merit figure was adjusted to provide robust solutions with large reactive loads and capacitor banks in the system, solving one of the problems encountered by Glamocanin.

5. A method to isolate failed components has been developed and customized to the data structures in EPRI's DEWorkstation.

6. The network load flow solution provides a lower bound on the losses, and a measure of how good the algorithm solution is. This would be a useful addition to other methods, since none can guarantee a global optimum.

7. The implementation allows a user to manually operate and lock switches before the algorithm runs. This would also be a useful addition to other methods.

Since this algorithm has been implemented in EPRI's DEWorkstation, it is ready for application by electric utilities in real-world situations. Future work should take further advantage of the integrated design environment in DEWorkstation:

1. The algorithm could include overcurrent protective coordination constraints, once the DEWorkstation's overcurrent protection application has a suitable programming interface.

2. The algorithm could include service reliability indices in the merit figure, once the DEWorkstation reliability application has been developed.

When the algorithm backtracks, or encounters a voltage or current constraint, this indicates an area where new equipment may improve the solution. Considerable design judgment is still required to select and size the new equipment. A new feature planned for DEWorktation will incorporate the output from a variety of applications, such as reconfiguration, capacitor placement, overcurrent protection, and reliablity analysis. The reconfiguration algorithm could be interfaced to this new integrated design tool, as it is developed.

Appendix A

User Manual

This appendix describes the user interface for the DAOP reconfiguration algorithm as implemented in DEWorkstation. The material is taken from the on-line help developed for the application, supplemented by screen shots from DEWorkstation and the DAOP reconfiguration application.

The application is installed by copying ***lossmin.dll*** to the DEWorkstation directory, and ***lossmin.hlp*** to the DEWorkstation help directory. The application has been named "loss minimization" to distinguish it from another DEWorkstation reconfiguration algorithm, which is based entirely on heuristics. Figure A.1 shows the DAOP reconfiguration algorithm selected to run, in DEWorkstation's application setup dialog.

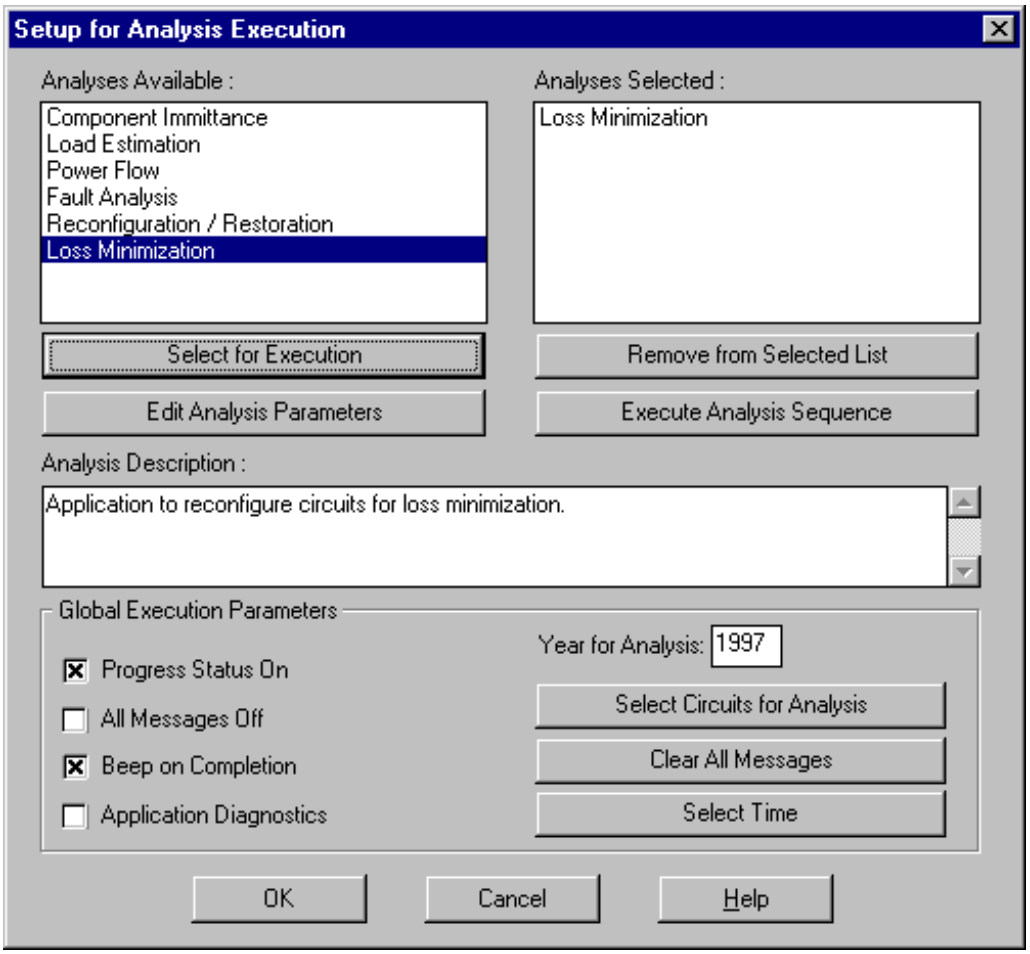

Figure A.1 - Loss minimization algorithm selected to run in DEWorkstation

A.1 Introduction to Loss Minimization

This application reconfigures the system switches for minimum losses, using the method of discrete ascent optimal programming (DAOP). Before the analysis runs, the user may specify failed components, and the algorithm will determine which switches must be opened to isolate these failed components. The user may also specify certain switches to lock open or closed, and the algorithm will not operate these switches.

After these preliminaries, the algorithm performs a power flow solution to determine the losses in the existing configuration. Then a network power may be performed with all operable switches closed. This determines the minimum possible loss, and provides a measure of how good the DAOP solution is compared to the existing configuration.

The DAOP solution commences by opening all operable switches, so that no load is served. Or, the user might wish to lock many of the existing switches in their present state, running DAOP on just a portion of the system. In that case the initial load served is not zero, but some base level.

Then DAOP proceeds in steps of closing one switch at a time, increasing the total load served and the total losses at each step, until all the load possible has been served. During this process the system is kept radial, and all voltage and current constraints are respected.

The DAOP method is a greedy search with some heuristic modifications. As such it should provide a good but not necessarily optimum solution. Compared to other methods of optimal switch reconfiguration, the main advantages of DAOP are more robust handling of constraints, and full nonlinear system analysis - leading to better accuracy.

A.2 Interactive Inputs - Loss Minimization

The analysis setup dialog for loss minimization, shown in Figure A.2, lets you specify which kinds of switches to operate, and what the voltage and current constraints will be. Specifying any failed components or locked switches is done later, using the control center.

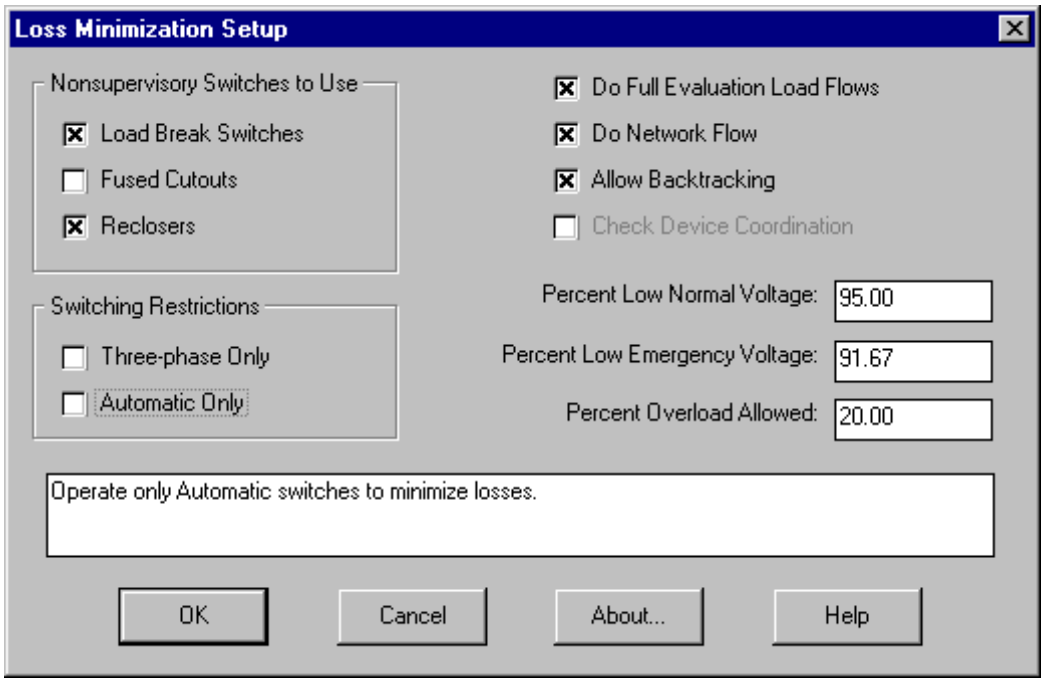

Figure A.2 - Setup dialog for loss minimization application

Nonsupervisory Switches To Use - This group of checkboxes allows you to specify that load break switches, fused cutouts, and/or reclosers are operable. If a box is unchecked, the algorithm will lock all switches of that class in the existing position. These choices interact with the Switching Restrictions checkboxes. Also, supervisory switches are always used.

Switching Restrictions - These checkboxes are optional. If ***three-phase only*** is checked, all single phase switches will be locked in their existing positions. If ***automatic only*** is checked, only supervisory switches or those that have an attached communications receiver will be operated in the algorithm.

The algorithm chooses switches to use as follows:

1. exclude all switches with ***Allow Device Movement*** turned off from the Schematic Control Center
2. exclude all switches operated using ***Lock Switches*** from the Loss Minimization Control Center
3. if ***three-phase only*** has been selected, exclude all single-phase and two-phase switches
4. of those remaining, all supervisory switches are used
5. nonsupervisory switches are also used if:
    a. their type matches a selected checkbox for load break switches, fused cutouts, or recloser

b. if ***automatic only*** has been selected, an attached communications receiver is also required

Do Full Evaluation Load Flows - If selected, each candidate switch closing is evaluated using the full radial power flow on that circuit. If not selected, short-cut calculations are used to screen each candidate and the full radial power flow is done only on the apparent best switch closing. The short-cut calculations run significantly faster and will not allow a switch closing that violates any constraints (because of the verifying radial power flow calculation). However, there is some risk that a best switch closing will be screened out due to apparent constraint violations that would not actually occur in a full radial power flow solution.

Do Network Flow - If selected, all switches to use are closed to obtain a lower bound on the losses. Closing all switches will typically create loops, requiring a network power flow solution. Due to topology assumptions of the network power flow, it may not be possible to close all switches and convergence may be difficult.

Allow Backtracking - If selected, the algorithm will keep track of alternate tie switches each time it completes an open loop. If more load is added to the open loop, these alternate ties will be re-evaluated. This option improves the algorithm's performance with, usually, a negligible increase in computational effort.

Check Device Coordination - If selected, the algorithm will check that overcurrent protective devices remain coordinated at each step. Note that voltage, current, and radiality constraints are always checked.

Percent Low Normal Voltage - Switching operations that allow any voltage to drop below this value are disallowed, under ***normal*** operating conditions.

Percent Low Emergency Voltage - Switching operations that cause any voltage to drop below this value are disallowed, under ***emergency*** operating conditions. The selection of normal or emergency condition is made later, using the control center.

Percent Overload Allowed - Switching operations that cause any component current overload to exceed this value are disallowed, under ***emergency*** operating conditions. The allowed current overload for ***normal*** conditions is 0%.

A.3 Control Center - Loss Minimization

When the loss minimization algorithm runs, the control center shown in Figure 20 appears in a floating window. The control center allows you to select normal or emergency ratings, specify any failed components, operate switches, start the analysis, and view results. Some of the buttons in Figure A.3 are not enabled until you run the algorithm.

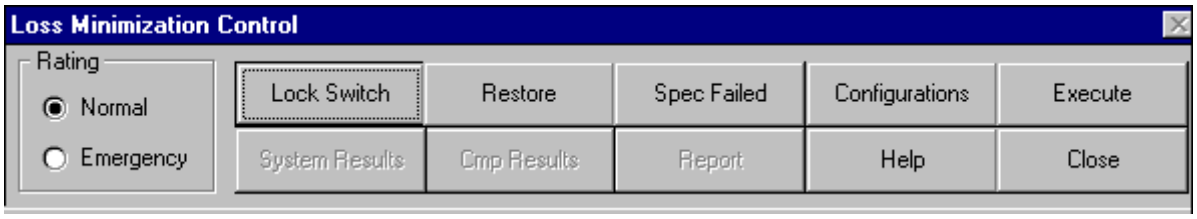

Figure A.3 - Control dialog for loss minimization - before execution

Any switches that had ***Allow Device Movement*** turned off in the Schematic Control Center will be highlighted with a gray ellipse on the schematic. Any switches manually operated through the control center's ***Lock Switches*** button will be highlighted with a magenta ellipse on the schematic. None of these switches will be operated automatically by the DAOP algorithm; they will be fixed in their existing positions when you select ***Execute***. The highlighting is removed when you close the Loss Minimization Control Center, but note that switches with the gray highlights are still locked for other DEW algorithms.

Normal/Emergency - These radiobuttons determine whether normal or emergency component current ratings are used as constraints, and also whether the normal or emergency low voltage constraint is used. Current ratings are established from the parts tables and voltage ratings are established from the setup panel.

Lock Switches - The chooser cursor appears to manually operate switches. Each time you click on a switch, the state toggles through:

1. locked in the original state
2. toggled from the original state and locked
3. automatically operable in the original state

Press ***Esc*** to exit this mode. Switches remain locked only for the loss minimization algorithm.

Restore - Return switch states and failed component states to their original condition, before invoking the control center.

Spec Failed - The chooser cursor appears to select failed components. Each time you click on a component, the state toggles between failed and good. Press ***Esc*** to exit this mode.

Configurations - Access the switching configurations dialog, which lets you save and restore various switch configurations (but not failed component selections).

Execute - Run the algorithm to isolate any failed components and reconfigure the switches for minimum loss. This enables the result buttons, as shown in Figure A.4.

Figure A.4 - Control dialog for loss minimization - after execution

System Result - Brings up a dialog showing the algorithm's recommended switches to open and close, with a command button to highlight each switch.

Cmp Result - The chooser cursor appears to select components for individual power flow results and messages. Press ***Esc*** to exit this mode.

Report - Formats a report of system results to save to disk, or view in Notepad.

A.4 Switching Configurations - Loss Minimization

The open/close state of each switch in the system can be saved and recalled using the dialog shown in Figure A.5. A switch configuration comprises a list of all switches in the system by name, with their current states.

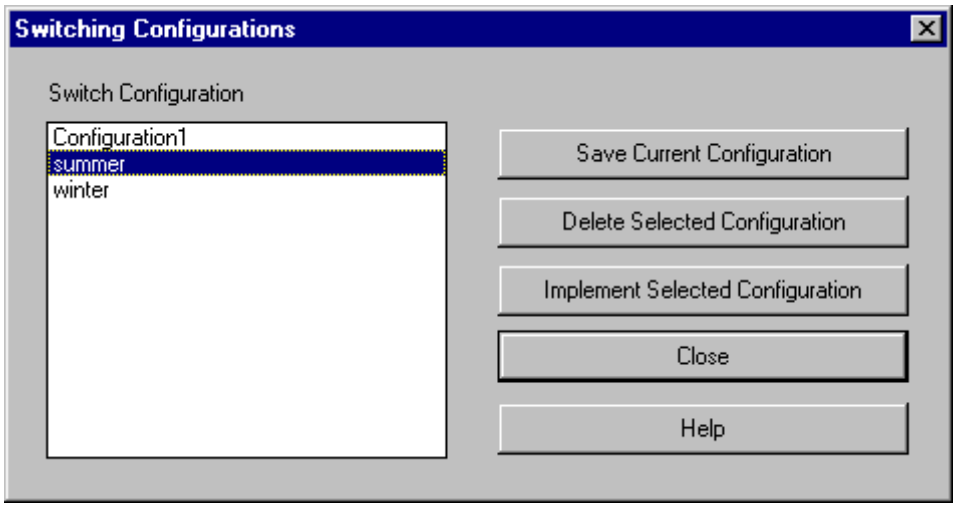

Figure A.5 - Dialog to manage switching configurations

Switch Configurations - This list shows all of the switch configurations you have saved by name. Select one from this list to recall or delete it.

Save Current Configuration - A dialog appears for you to supply a unique name. All existing switch states will be saved as a configuration under this name.

Delete Selected Configuration - Delete the selected configuration.

Implement Selected Configuration - Set all switches to the states specified in the selected configuration.

A.5 Outputs - Loss Minimization

The loss minimization algorithm produces four kinds of output:

Switch Configuration - Operable switches will be opened or closed to isolate failed components and minimize losses. The switch configuration may be viewed on the schematic, and saved using the switching configurations dialog accessed through the control center.

System Results - A list of switches operated by the algorithm is displayed in a listbox, segregated by those operated to isolate failed components and those operated to minimize losses. Figure A.6 shows the dialog used to display the switching operations. The ***Pan*** button centers and highlights the selected switch on the schematic.

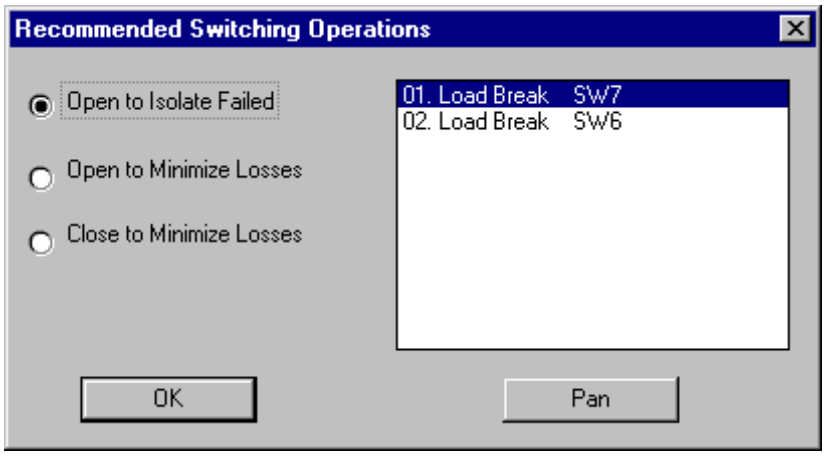

Figure A.6 - Switching operation results dialog for loss minimization

Component Results - Individual component results include those available from the final power flow solution. There may also be messages on certain components reaching constraints.

Text Files - The formatted text output includes system losses and unserved loads for the initial system, DAOP solution, and network system. Figure A.7 shows a sample text report. In each of the three reported systems, any failed components have been isolated already by opening switches. The network system's numbers will be zero, unless the user requested a network power flow in the setup panel.

The formatted text output also lists the switches to open or close, separately for isolating failed components and for minimizing the subsequent losses. If the user specified failed componentes, or manually locked any switches from the control center, those components are also listed.

The algorithm also writes a text file called ***lm_times.txt*** in DEWorkstation's directory. This file is written each time DAOP runs. It shows the time spent in full power flow calculations, approximate loss evaluations, network power flow, and open-loop backtracking.

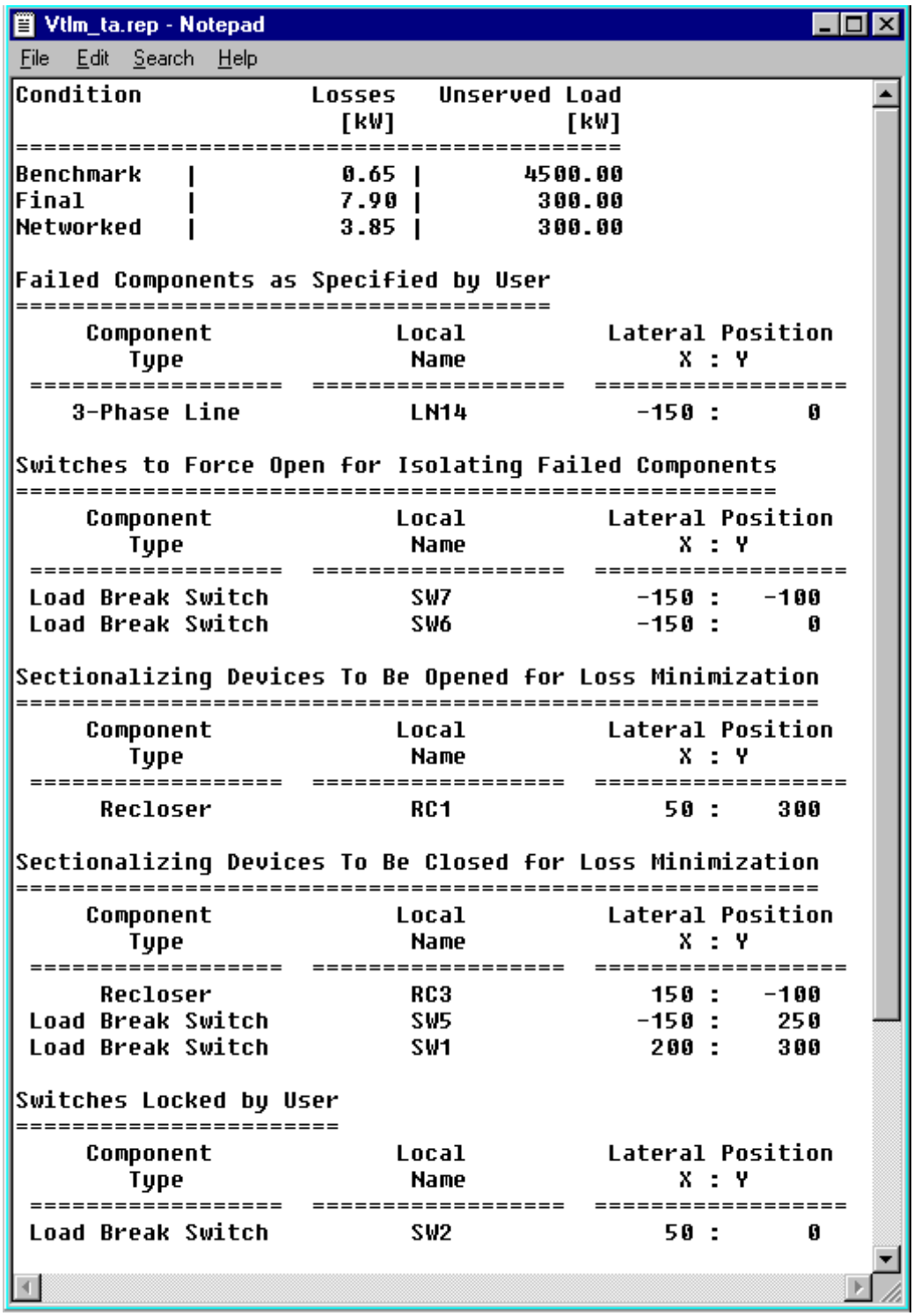

Figure A.7 - Sample report from loss minimization

Appendix B

Derivation of Approximate Loss Equation

This appendix presents a derivation of the approximate loss equation (3.2). The system losses occur in overhead lines, cables, transformers, and other series-connected devices. Figure B.1 shows a three-phase line or transformer, with its series impedance separated into real and imaginary parts. The phase currents, denoted $\mathbf{I}_1$, $\mathbf{I}_2$, and $\mathbf{I}_3$, create a series voltage drop in the device. To calculate the real power loss, we only need the resistive part of the series voltage drop in each phase, which is denoted $\mathbf{V}_1$, $\mathbf{V}_2$, and $\mathbf{V}_3$ in Figure B.1. The phase conductors are coupled, so that both R and X are three-by-three matrices. The currents and voltages are both phasor quantities, while R is real.

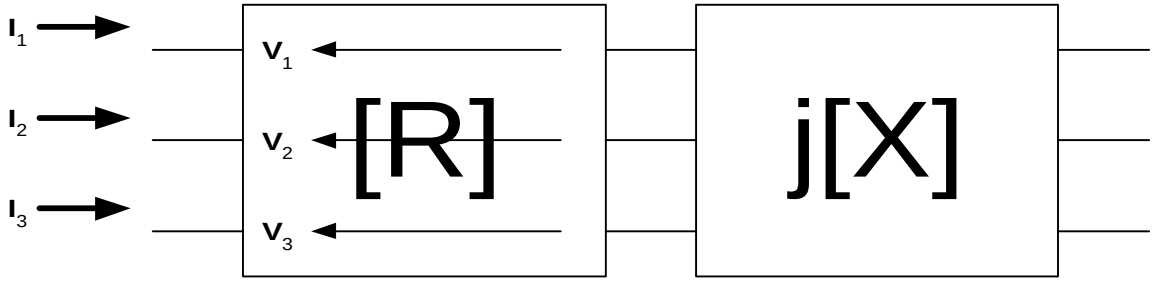

Figure B.1 - A three-phase lossy device.

The real power loss is given by the complex power equation, (B.1). Even though this is a phasor expression, note that the result should be a real number.

$$\boldsymbol{S} = \boldsymbol{I}_1 \boldsymbol{V}_1^* + \boldsymbol{I}_2 \boldsymbol{V}_2^* + \boldsymbol{I}_3 \boldsymbol{V}_3^* \tag{B.1}$$

We can replace the voltages in (B.1) with an expansion of the resistance matrix multiplication:

$$\boldsymbol{S} = \boldsymbol{I}_1 (R_{11}\boldsymbol{I}_1^* + R_{12}\boldsymbol{I}_2^* + R_{13}\boldsymbol{I}_3^*) + \boldsymbol{I}_2 (R_{21}\boldsymbol{I}_1^* + R_{22}\boldsymbol{I}_2^* + R_{23}\boldsymbol{I}_3^*) + \boldsymbol{I}_3 (R_{31}\boldsymbol{I}_1^* + R_{32}\boldsymbol{I}_2^* + R_{33}\boldsymbol{I}_3^*) \tag{B.2}$$

The R matrix is symmetric, so that $R_{12} = R_{21}$, $R_{13} = R_{32}$, and $R_{23} = R_{32}$. Rearranging the terms in (B.2), we obtain:

$$\boldsymbol{S} = R_{11}\boldsymbol{I}_1\boldsymbol{I}_1^* + R_{22}\boldsymbol{I}_2\boldsymbol{I}_2^* + R_{33}\boldsymbol{I}_3\boldsymbol{I}_3^* + R_{12}(\boldsymbol{I}_1\boldsymbol{I}_2^* + \boldsymbol{I}_2\boldsymbol{I}_1^*) + R_{13}(\boldsymbol{I}_1\boldsymbol{I}_3^* + \boldsymbol{I}_3\boldsymbol{I}_1^*) + R_{23}(\boldsymbol{I}_2\boldsymbol{I}_3^* + \boldsymbol{I}_3\boldsymbol{I}_2^*) \tag{B.3}$$

The product of a phasor current and its conjugate is the magnitude squared, denoted I^2, so:

$$\boldsymbol{S} = R_{11}I_1^2 + R_{22}I_2^2 + R_{33}I_3^2 + R_{12}(\boldsymbol{I}_1\boldsymbol{I}_2^* + \boldsymbol{I}_2\boldsymbol{I}_1^*) + R_{13}(\boldsymbol{I}_1\boldsymbol{I}_3^* + \boldsymbol{I}_3\boldsymbol{I}_1^*) + R_{23}(\boldsymbol{I}_2\boldsymbol{I}_3^* + \boldsymbol{I}_3\boldsymbol{I}_2^*) \tag{B.4}$$

The first three terms in (B.4) are real, and account for the resistive loss in each conductor with no coupling. Each of the three cross terms will also reduce to a real number, as shown for two arbitrary phasors, **A** and **B**, in (B.5).

$$\begin{aligned} \boldsymbol{AB}^* + \boldsymbol{BA}^* &= (A_{re} + jA_{im})(B_{re} - jB_{im}) + (B_{re} + jB_{im})(A_{re} - jA_{im}) \\ &= A_{re}B_{re} + A_{im}B_{im} + jA_{im}B_{re} - jA_{re}B_{im} + A_{re}B_{re} + A_{im}B_{im} + jA_{re}B_{im} - jA_{im}B_{re} \\ &= 2(A_{re}B_{re} + A_{im}B_{im}) \end{aligned} \quad \text{(B.5)}$$

By defining complex decompositions of the phase currents in (B.6)-(B.8), we can write the real power loss in (B.9).

$$\boldsymbol{I}_1 \equiv A_{re} + jA_{im} \quad \text{(B.6)}$$

$$\boldsymbol{I}_2 \equiv B_{re} + jB_{im} \quad \text{(B.7)}$$

$$\boldsymbol{I}_3 \equiv C_{re} + jC_{im} \quad \text{(B.8)}$$

$$P = I_1^2R_{11} + I_2^2R_{22} + I_3^2R_{33} + 2R_{12}(A_{re}B_{re} + A_{im}B_{im}) + 2R_{13}(A_{re}C_{re} + A_{im}C_{im}) + 2R_{23}(B_{re}C_{re} + B_{im}C_{im}) \quad \text{(B.9)}$$

Equation (B.9) is quite similar to (3.2), except for the prime superscripts in (3.2) indicating a modified current phase reference. To use (B.9), we can estimate the current in each phase independently, in (B.10)-(B.15).

$$A_{re} = kWflow_1/kV_1 \quad \text{(B.10)}$$

$$A_{im} = kVARflow_1/kV_1 \quad \text{(B.11)}$$

$$B_{re} = kWflow_2/kV_2 \quad \text{(B.12)}$$

$$B_{im} = kVARflow_2/kV_2 \quad \text{(B.13)}$$

$$C_{re} = kWflow_3/kV_3 \quad \text{(B.14)}$$

$$C_{im} = kVARflow_3/kV_3 \quad \text{(B.15)}$$

The real and reactive power flows in (B.10)-(B.15) are known from the system load models, which generally specify the load in real and reactive power. The total downstream real and reactive load served by each line segment or transformer is summed to obtain the flows, and then any downstream capacitor banks are subtracted from the reactive power flow. The phase-to-ground voltage magnitudes in (B.10)-(B.15) are obtained from the most recent load flow solution. Note these voltages are not the series voltage drops $\mathbf{V}_1$, $\mathbf{V}_2$, and $\mathbf{V}_3$ shown in Figure B.1.

The three phase currents estimated in (B.10)-(B.15) have phase angles referenced to their individual phase-to-ground voltages. To use these estimated currents in (B.9), they must be converted to the same phase reference. The three phase-to-ground voltages will have phase differences of approximately 120 degrees. Unbalanced source voltages, loads, or line impedances may cause variations of a few degrees in the voltage phase angles, but usually the difference is less than one degree. (The currents will often be much more unbalanced than the voltages.) The phase 1 voltage is arbitrarily chosen to be the phase reference at zero degrees, in (B.16). We then assume phase 2 lags phase 1 by 120 degrees (B.17) and that phase 3 leads phase 1 by 120 degrees (B.18).

$$\boldsymbol{I}_1^{'} = (A_{re} + jA_{im}) \tag{B.16}$$

$$\boldsymbol{I}_2^{'} = (B_{re} + jB_{im})(-\tfrac{1}{2} - j\tfrac{\sqrt{3}}{2}) = -\tfrac{1}{2}B_{re} + \tfrac{\sqrt{3}}{2}B_{im} - j\tfrac{1}{2}B_{im} - j\tfrac{\sqrt{3}}{2}B_{re} \tag{B.17}$$

$$\boldsymbol{I}_3^{'} = (C_{re} + jC_{im})(-\tfrac{1}{2} + j\tfrac{\sqrt{3}}{2}) = -\tfrac{1}{2}C_{re} - \tfrac{\sqrt{3}}{2}C_{im} - j\tfrac{1}{2}C_{im} + j\tfrac{\sqrt{3}}{2}C_{re} \tag{B.18}$$

A new set of estimated currents, rotated to the same phase reference, is given in (B.19)-(B.24).

$$A_{re}^{'} = A_{re} \tag{B.19}$$

$$A_{im}^{'} = A_{im} \tag{B.20}$$

$$B_{re}^{'} = -0.5B_{re} + 0.866B_{im} \tag{B.21}$$

$$B_{re}^{'} = -0.5B_{im} - 0.866B_{re} \tag{B.22}$$

$$C_{re}^{'} = -0.5C_{re} - 0.866C_{im} \tag{B.23}$$

$$C_{re}^{'} = -0.5C_{im} + 0.866C_{re} \tag{B.24}$$

Replacing the currents in (B.9) with (B.19)-(B.24), we obtain (3.2).

The approximate loss formula is applied to components energized by a candidate switch, and also to components in the feeder path from the candidate switch back to the source. These feeder path components have a current increase due to the additional load. Another approximate loss formula was developed for the loss increment in the feeder path components, but it proved more efficient to apply (3.2) to the incremented feeder path currents, and then subtract the pre-switching losses as determined from the existing load flow solution.

References

Abdel-Salam, T. S., A. Y. Chikhani and R. Hackam, "A New Technique for Loss Reduction Using Compensating Capacitors Applied to Distribution Systems with Varying Load Condition", *IEEE Transactions on Power Delivery,* 9-2, April 1994, pp. 819-827.

Alsac, O., J. Bright, M. Prais and B. Stott, "Further Developments in LP-Based Optimal Power Flow", *IEEE Transactions on Power Systems,* 5-3, August 1990, pp. 697-706.

Aoki, K., T. Ichimori and M. Kanezashi, "Normal State Optimal Load Allocation in Distribution Systems", *IEEE Transactions on Power Delivery,* 2-1, January 1987, pp. 147-155.

Aoki, K., T. Satoh, H. Itoh, H. Kuwabara and M. Kanezashi, "Voltage Drop Constrained Restoration of Supply by Switch Operation in Distribution Systems", *IEEE Transactions on Power Delivery,* 3-3, July 1988, pp. 1267-1274.

Aoki, K., H. Kuwabara, T. Satoh and M. Kanezashi, "An Efficient Algorithm for Load Balancing of Transformers and Feeders by Switch Operation in Large Scale Distribution Systems", *IEEE Transactions on Power Delivery,* 3-4, October 1988, pp. 1865-1872.

Aoki, K., K. Nara, M. Itoh, T. Satoh and H. Kuwabara, "A New Algorithm for Service Restoration in Distribution Systems", *IEEE Transactions on Power Delivery,* 4-3, July 1989, pp. 1832-1839.

Aoki, K., K. Nara, T. Satoh, M. Itoh and H. Kuwabara, M. Kitagawa, K. Yamanaka, "Totally Automated Switching Operation in Distribution System", *IEEE Transactions on Power Delivery,* 5-1, January 1990, pp. 514-520.

Aoki, K., K. Nara, T. Satoh, M. Kitagawa and K. Yamanaka, "New Approximate Optimization Method for Distribution System Planning", *IEEE Transactions on Power Systems,* 5-1, February 1990, pp. 126-132.

Augugliaro, A., L. Dusonchet and S. Mangione, "Optimal Reconfiguration of Distribution Network for Loss Reduction Using Non-linear Programming", ETEP l-6, pp. 317-323, November/December 1991.

Bae, Y. G., "Analytical Method of Capacitor Allocation on Distribution Primary Feeders", *IEEE Transactions on Power Apparatus & Systems,* 97-4, July/August 1978, pp. 1232-1238.

Baghzouz, Y., "Effects of Nonlinear Loads on Optimal Capacitor Placement in Radial Feeders", *IEEE Transactions on Power Delivery,* 6-1, January 1991, pp. 245-251.

Baldick, R. and F. F. Wu, "Efficient Integer Optimization Algorithms for Optimal Coordination of Capacitors and Regulators", *IEEE Transactions on Power Systems,* 5-3, August 1990, pp. 805-812.

Baldick, R. and F. F. Wu, "Approximation Formulas for the Distribution System: the Loss Function and Voltage Dependence", *IEEE Transactions on Power Delivery,* 6-1, January 1991 pp. 252-259.

Baran, M. E. and F. F. Wu, "Optimal Capacitor Placement on Radial Distribution Systems", *IEEE Transactions on Power Delivery*, 4-1, January 1989, pp. 725-734.

Baran, M. E. and F. F. Wu, "Optimal Sizing of Capacitors Placed on a Radial Distribution System", *IEEE Transactions on Power Delivery*, 4-1, January 1989, pp. 735-743.

Baran, M. E. and F. F. Wu, "Network Reconfiguration in Distribution Systems for Loss Reduction and Load Balancing", *IEEE Transactions on Power Delivery*, 4-2, April 1989, pp. 1401-1407.

Billinton, R. and S. Jonnavithula, "Optimal Switching Device Placement in Radial Distribution Systems," *IEEE Transactions on Power Delivery*, 11-3, July 1996, pp. 1646-1651.

Bishop, M. T. and R. E. Lee, "Distribution System Line Loss Reduction Through Enhanced Capacitor Location Techniques", *IEEE Transactions on Power Delivery*, 1-2, April 1986, pp. 190-197.

Blair, W. E., J. B. Bunch and C. H. Gentz, "A Methodology for Economic Evaluation of Distribution Automation", *IEEE Transactions on Power Apparatus & Systems*, 104-10, October 1985, pp. 2954-2960.

Boardman, J. T. and C. C. Meckiff, "A Branch and Bound Formulation to an Electricity Distribution Planning Program", *IEEE Transactions on Power Apparatus & Systems*, 104-8, August 1985, pp. 2112-2118.

Borowski, D. and R. Seamon, "EPRI Project RP 2592, Large Scale Distribution Automation and Load Control, Enters Test Year", *IEEE Transactions on Power Delivery*, 5-1, January 1990, pp. 486-492.

Borozan, V., D. Rajicic and R. Ackovski, "Improved Method for Loss Minimization in Distribution Networks," *IEEE Transactions on Power Systems*, 10-3, August 1995, pp. 1420-1425.

Broadwater, R. P., J. C. Thompson, R. E. Lee and H. Maghdan, "Computer-Aided Protection Ssytem Design with Reconfiguration", *IEEE Transactions on Power Delivery*, 6-1, January 1991, pp. 260-266.

Broadwater, R. P., A. H. Khan, H. E. Shaalan and R. E. Lee, "Time Varying Load Analysis to Reduce Distribution Losses Through Reconfiguration", *IEEE Transactions on Power Delivery*, 8-1, January 1993, pp. 294-300.

Broadwater, R., J. Thompson, M. Ellis, H. Ng, D. Loyd, "Application Programmer Interface for the EPRI Distribution Engineering Workstation", *IEEE Transactions on Power Systems*, 10-1, February 1995, pp. 499-505.

Broadwater, R. P., P. A. Dolloff, T. L. Herdman, R. Karamikhova and A. Sargent, "Minimum Loss Optimization in Distribution Systems: Discrete Ascent Optimal Programming", *Electric Power Systems Research*, vol. 36, 1996, pp. 113-121.

Bunch, J. B., R. D. Miller and J. E. Wheeler, "Distribution System Integrated Voltage and Reactive Power Control", *IEEE Transactions on Power Apparatus & Systems*, 101-2, February 1982, pp. 284-289.

Bunch, J. B., L. A. Demian, C. H. Gentz, K. J. Tanis and H. J. Fiedler, "A Distribution Automation Evaluation Using Digital Techniques", *IEEE Transactions on Power Apparatus & Systems,* 104-11, November 1985, pp. 3169-3175.

Cassel, W. R., "Distribution Management Systems: Functions and Payback", *IEEE Transactions on Power Systems,*, August 1993, pp. 796-801.

Castro, C. H., J. B. Bunch and T. M. Topka, "Generalized Algorithms for Distribution Feeder Deployment and Sectionalizing", *IEEE Transactions on Power Apparatus & Systems,* 99-2, March/April 1980, pp. 549-557.

Cespedes, R., "New Method for the Analysis of Distribution Systems", *IEEE Transactions on Power Delivery,* 5-1, January 1990, pp. 391-396.

Chang, H.-C. and Ch.-Ch. Kuo, "Network Reconfiguration in Distribution Systems using Simulated Annealing", *Electric Power Systems Research,* vol. 29, pp. 227-238, 1994.

Chiang, H.-D. and R. Jean-Jumeau, "Optimal Network Reconfigurations in Distribution Systems: Part 1: A New Formulation and A Solution Methodology", *IEEE Transactions on Power Delivery,* 5-4, November 1990, pp. 1902-1909.

Chen, C. S. and M. Y. Cho, "Determination of Critical Switches in Distribution System," PWRD-7-3, July 1992, pp. 1443-1449.

Cheng, C. S. and D. Shirmohammadi, "A Three-Phase Power Flow Method for Real-Time Distribution System Analysis," *IEEE Transactions on Power Systems,* 10-2, May 1995, pp. 671-679.

Civanlar, S., J. J. Grainger, Y. Yin and S. S. Lee, "Distribution Feeder Reconfiguration for Loss Reduction", *IEEE Transactions on Power Delivery,* 3-3, July 1988, pp. 1217-1223.

Deo, N., *Graph Theory with Applications to Engineering and Computer Science*, Prentice-Hall, 1974.

Desai, K. and D. R. Brown, "Multiple Variable Sources of Reactive Power on Distribution System Primary Feeders", *IEEE Transactions on Power Apparatus & Systems,* 101-12, December 1982, pp. 4674-4680.

Devi, V. S., D. P. Sen Gupta and G. Anandalingam, "Optimal Restoration of Power Supply in Large Distribution Systems in Developing Countries," *IEEE Transactions on Power Delivery,* 10-1, January 1995, pp. 430-438.

Dolloff, P. A., *Optimization in Electrical Distribution Systems: Discrete Ascent Optimal Programming*, Ph.D. Thesis, Virginia Polytechnic Institute and State University, December 1995.

Dommel, H. W. and W. F. Tinney, "Optimal Power Flow Solutions", *IEEE Transactions on Power Apparatus & Systems,* 87-10, October 1968, pp. 1866-1876.

El-Kib, A. A., J. J. Grainger, K. N. Clinard and L. J. Gale, "Placement of Fixed and/or Non-Simultaneously Switched Capacitors on Unbalanced Three-Phase Feeders Involving

Laterals", *IEEE Transactions on Power Apparatus & Systems,* 104-11, November 1985, pp. 3298-3305.

EPRI, *Distribution Engineering Workstation Volume 5: Data Schema, Version 1.01*, Report Number EL-7249-V5, Electric Power Research Institute, Palo Alto, CA, September 1995.

Fan, J.-Y., L. Zhang and J. D. McDonald, "Distribution Network Reconfiguration: Single Loop Optimization," *IEEE Transactions on Power Systems,* 11-3, August 1996, pp. 1643-1647.

Fawzi, T. H., S. M. El-Sobki and M. A. Abdel-Halim, "New Approach for the Application of Shunt Capacitors to the Primary Distribution Feeders", *IEEE Transactions on Power Apparatus & Systems,* 102-1, January 1983, pp. 10-13.

Fernandes, R. A., F. A. Rushden, J. B. Bunch, H. Chestnut, J. H. Easley and H. J. Fiedler, "Evaluation of a Conceptual Distribution Automation System", *IEEE Transactions on Power Apparatus & Systems,* 101-7, July 1982, pp. 2024-2031.

Glamocanin, V., "Optimal Loss Reduction of Distribution Networks", *IEEE Transactions on Power Systems,* 5-3, August 1990, pp. 774-781.

Glamocanin, V. and V. Filipovic, "Open Loop Distribution System Design", *IEEE Transactions on Power Delivery,* 8-4, October 1993, pp. 1900-1906.

Gonen, T. and A. A. Mahmoud, "Bibliography of Power Distribution System Planning", *IEEE Transactions on Power Apparatus & Systems,* 102-6, June 1983, pp. 1778-1787.

Goswami, S. K. and S. K. Basu, "A New Algorithm for the Reconfiguration of Distribution Feeders for Loss Minimization", *IEEE Transactions on Power Delivery,* 7-3, July 1992, pp. 1484-1491.

Grainger, J. J. and S. H. Lee, "Optimum Size and Location of Shunt Capacitors for Reduction of Losses on Distribution Feeders", *IEEE Transactions on Power Apparatus & Systems,* 100-3, March 1981, pp. 1105-1118.

Grainger, J. J. and S. H. Lee, "Capacity Release by Shunt Capacitor Placement on Distribution Feeders: A New Voltage-Dependent Model", *IEEE Transactions on Power Apparatus & Systems,* 101-5, May 1982, pp. 1236-1244.

Grainger, J. J., S. H. Lee and A. A. El-Kib, "Design of a Real-Time Switching Control Scheme for Capacitive Compensation of Distribution Feeders", *IEEE Transactions on Power Apparatus & Systems,* 101-8, August 1982, pp. 2420-2428.

Grainger, J. J., A. A. El-Kib and S. H. Lee, "Optimal Capacitor Placement on Three-Phase Primary Feeders: Load and Feeder Unbalance Effects", *IEEE Transactions on Power Apparatus & Systems,* 102-10, October 1983, pp. 3296-3305.

Grainger, J. J., S. Civanlar, K. N. Clinard and L. J. Gale, "Discrete-Tap Control Scheme for Capacitive Compensation of Distribution Feeders", *IEEE Transactions on Power Apparatus & Systems,* 103-8, August 1984, pp. 2098-2107.

Grainger, J. J., S. Civanlar, K. N. Clinard and L. J. Gale, "Optimal Voltage Dependent Continuous-Tome Control of Reactive Power on Primary Feeders", *IEEE Transactions on Power Apparatus & Systems*, 103-9, September 1984, pp. 2714-2722.

Grainger, J. J. and S. Civanlar, "Volt/Var Control on Distribution Systems with Lateral Branches Using Shunt Capacitors and Voltage Regulators Part I: The Overall Problem", *IEEE Transactions on Power Apparatus & Systems*, 104-11, November 1985, pp. 3278-3283.

Grainger, J. J. and S. Civanlar, "Volt/Var Control on Distribution Systems with Lateral Branches Using Shunt Capacitors and Voltage Regulators Part II: The Solution Method", *IEEE Transactions on Power Apparatus & Systems*, 104-11, November 1985, pp. 3284-3290.

Grainger, J. J. and S. Civanlar, "Volt/Var Control on Distribution Systems with Lateral Branches Using Shunt Capacitors and Voltage Regulators Part III: The Numerical Results", *IEEE Transactions on Power Apparatus & Systems*, 104-11, November 1985, pp. 3291-3297.

Happ, H. H. and K. A. Wirgau, "Static and Dynamic VAR Compensation in System Planning", *IEEE Transactions on Power Apparatus & Systems*, 97-5, September/October 1978, pp. 1564-1578.

Hayashi, Y., S. Iwamoto, S. Furuya and C.-C. Liu, "Efficient Determination of Optimal Radial Power System Structure Using Hopfield Neural Network with Constrained Noise," *IEEE Transactions on Power Delivery*, 11-3, July 1996, pp. 1529-1535.

Hsu, Y.-Y., H. M. Huang, H. C. Kuo, S. K. Peng, C. W. Chang, K. J. Chang, H. S. Yu, C. E. Chow and R. T. Kuo, "Distribution System Service Restoration Using a Heuristic Search Approach", *IEEE Transactions on Power Delivery*, 7-2, April 1992, pp. 734-740.

Hsu, Y.-Y., J.-H. Yi, S. S. Liu, Y. W. Chen. H. C. Feng and Y. M. Lee, "Transformer and Feeder Load Balancing Using Heuristic Search Approach", *IEEE Transactions on Power Systems*, 8-1, February 1993, pp. 184-190.

Hsu, Y.-Y. and Y. Jwo-Hsu, "Planning of Distribution Feeder Reconfiguration with Protective Device Coordination", *IEEE Transactions on Power Delivery*, 8-3, July 1993, pp. 1340-1347.

Hsu, Y.-Y. and H. C. Kuo, "A Heuristic Based Fuzzy Reasoning Approach for Distribution System Service Restoration", *IEEE Transactions on Power Delivery*, 9-2, April 1994, pp. 948-953.

Hsu, Y.-Y. and C.-C. Yang, "A Hybrid Artificial Neural Network-Dynamic Programming Approach for Feeder Capacitor Scheduling", *IEEE Transactions on Power Systems*, 9-2, May 1994, pp. 1069-1075.

Huddleston, C. T., R. P. Broadwater and A. Chandrasekaran, "Reconfiguration Algorithm for Minimizing Losses in Radial Electric Distribution Systems", *Electric Power Systems Research*, vol. 18, 1990, pp. 57-66.

IEEE Task Group on Long Range Distribution System Design, "The Distribution System of the Year 2000", *IEEE Transactions on Power Apparatus & Systems*, 101-8, August 1982, pp. 2485-2490.

IEEE Task Group on State of the Art Distribution System Design, "Bibliography on Distribution Automation", *IEEE Transactions on Power Apparatus & Systems,* 103-6, June 1984, pp. 1176-1182.

IEEE Distribution Planning Working Group, "Radial Distribution Test Feeders", *IEEE Transactions on Power Systems,* 6-3, August 1991, pp. 975-985.

Iyer, S. R., K. Ramachandran and S. Hariharan, "Optimal Reactive Power Allocation for Improved System Performance", *IEEE Transactions on Power Apparatus & Systems,* 103-6, June 1984, pp. 1509-1515.

Jiang, D. and R. Baldick, "Optimal Electric Distribution System Switch Reconfiguration and Capacitor Control," *IEEE Transactions on Power Systems,* 11-2, May 1996, pp. 890-897.

Jung, H.-H., H. Kim and Y. Ko, "Network Reconfiguration Algorithm for Automated Distribution Systems Based on Artificial Intelligence Approach", *IEEE Transactions on Power Delivery,* 8-4, October 1993, pp. 1933-1941.

Kaplan, M., "Optimization of Number, Location, Size, Control Type, and Control Setting of Shunt Capacitors on Radial Distribution Feeders", *IEEE Transactions on Power Apparatus & Systems,* 103-9, September 1984, pp. 2659-2665.

Kato, S., T. Naito, H. Kohno, H. Kanawa and T. Shoji, "Computer-Based Distribution Automation," PWRD-1-1, January 1986, pp. 265-271.

Kendrew, T. J. and J. A. Marks, "Distribution Automation Comes of Age," *IEEE Computer Applications in Power,* 2-1, January 1989, pp. 7-10.

Kim, H., Y. Ko and K.-H. Jung, "Artificial Neural-Network Based Feeder Reconfiguration for Loss Reduction in Distribution Systems", *IEEE Transactions on Power Delivery,* 8-3, July 1993, pp. 1356-1366.

Lee, R. E. and C. L. Brooks, "A Method and its Application to Evaluate Automated Distribution Control", *IEEE Transactions on Power Delivery*, 3-3, July 1988, pp. 1232-1240.

Lee, S. H. and J. J. Grainger, "Optimum Placement of Fixed and Switched Capacitors on Distribution Primary Feeders", *IEEE Transactions on Power Apparatus & Systems,* 100-1, January 1981, pp. 345-352.

Lin, W.-M. and H.-C. Chin, "A New Approach for Distribution Feeder Reconfiguration for Loss Reduction and Service Restoration," IEEE paper PE-809-PWRD-0-06-1997, to be published.

Liu, C.-C., S. J. Lee and S. S. Venkata, "An Expert System Operational Aid Restoration and Loss Reduction of Distribution Systems", *IEEE Transactions on Power Systems,* 3-2, May 1988, pp. 619-626.

Liu, C.-C., S. J. Lee and K. Vu, "Loss Minimization of Distribution Feeders: Optimality and Algorithms", PWRD-4-2, pp. 1281-1289, April 1989.

Markushevich, N. S., I. C. Herejk and R. E. Nielson, "Functional Requirements and Cost-Benefit Study for Distribution Automation at B. C. Hydro", *IEEE Transactions on Power Systems,* 9-2, May 1994, pp. 772-781.

McCall, L. V. and B. J. Chambers, "Scarborough Distribution Automation Project Implementation and Preliminary Performance Experience", *IEEE Transactions on Power Apparatus & Systems,* 104-10, October 1985, pp. 2759-2763.

Michalewicz, Z., *Genetic Algorithms + Data Structures = Evolution Programs,* 2nd ed., Springer-Verlag, 1994.

Mikic, O. M., "Mathematical Dynamic Model for Long-Term Distribution System Planning", *IEEE Transactions on Power Systems,* 1-1, February 1986, pp. 34-40.

Miu, K. N., H.-D. Chiang, B. Yuan and G. Darling, "Fast Service Restoration for Large-Scale Distribution Systems with Priority Customers and Constraints", IEEE paper PE-004PWRS-16-09-1997, to be published.

Momoh, J. A., S. X. Guo, E. C. Ogbuobiri and R. Adapa, "The Quadratic Interior Point Method Solving Power System Optimization Problems", *IEEE Transactions on Power Systems,* 9-3, August 1994, pp. 1327-1336.

Morelato, A. L. and A.Monticelli, "Heuristic Search Approach to Distribution System Restoration", *IEEE Transactions on Power Delivery,* 4-4, October 1989, pp. 2235-2241.

Nagendra Rao, P. S. "An Extremely Simple Method of Determining Optimal Conductor Sections for Radial Distribution Feeders", *IEEE Transactions on Power Apparatus & Systems,* 104-6, June 1985, pp. 1439-1442.

Nara, K., A. Shiose, M. Kitagawa and T. Ishihara, "Implementation of Genetic Algorithm for Distribution Ssytem Loss Minimum Reconfiguration", *IEEE Transactions on Power Systems,* 7-3, August 1992, pp. 1044-1051.

Partanen, J., "A Modified Dynamic Programming Algorithm for Sizing, Locating, and Timing of Feeder Reinforcements", *IEEE Transactions on Power Delivery,* 5-1, January 1990, pp. 277-283.

Peponis, G. J., M. P. Papadopoulos and N. D. Hatziargyriou, "Distribution Network Reconfiguration to Minimize Line Losses," *IEEE Transactions on Power Systems,* 10-3, July 1995, pp. 1338-1342.

Peponis, G. J., M. P. Papadopoulos and N. D. Hatziargyriou, "Optimal Operation of Distribution Networks," *IEEE Transactions on Power Systems,* 11-1, January 1996, pp. 59-67.

Pierre, D. A., *Optimization Theory with Applications*, Dover Publications, 1986.

Ponnaveikko, M. and K. S. Prakasa Rao, "Optimal Choice of Fixed and Switched Shunt Capacitors on Radial Distributors by the Method of Local Variations", *IEEE Transactions on Power Apparatus & Systems,* 102-6, June 1983, pp. 1607-1615.

Ponnavaikko, N., K. S. Prakasa Rao and S. S. Venkata, "Distribution System Planning Through a Quadratic Mixed Integer Programming Approach", *IEEE Transactions on Power Delivery,* 2-4, October 1987, pp. 1157-1163.

Purucker, S. L., T. W. Reddoch, J. S. Detwiler and L. D. Monteen, "The Design of an Integrated Distribution Control System", *IEEE Transactions on Power Apparatus & Systems,* 104-3, March 1983, pp. 745-752.

Purucker, S. I., R. J. Thomas and L. D. Monteen, "Feeder Automation Designs for Installing an Integrated Distribution Control System", *IEEE Transactions on Power Apparatus & Systems,* 104-10, October 1985, pp. 2929-2934.

Raj, B. N. and K. S. P. Rao, "A New Fuzzy Reasoning Approach for Load Balancing in Distribution System," *IEEE Transactions on Power Systems,* 10-3, August 1995, pp. 1426-1432.

Rau, N. S. and Y.-H. Wan, "Optimum Location of Resources in Distributed Planning", *IEEE Transactions on Power Systems,* 9-4, November 1994, pp. 2014-2020.

Redmon, J. R. and C. B. Gentz, "Affect of Distribution Automation and Control on Future System Configuration", *IEEE Transactions on Power Apparatus & Systems,* 100-4, April 1981, pp. 1923-1931.

Rizy, D. T., J. S. Lawler, J. B. Patton and N. H. Fortson, "Distribution Automation Applications Software for the Athens Utilities Board", *IEEE Transactions on Power Delivery,* 4-1, January 1989, pp. 715-724.

Ross, D. W., J. Patton, A. I. Cohen and M. Carson, "New Methods for Evaluating Distribution Automation and Control (DAC) Systems Benefits", *IEEE Transactions on Power Apparatus & Systems,* 100-6, June 1981, pp. 2978-2986.

Roytelman, I. and S. M. Shahidehpour, "Practical Aspects of Distribution Automation in Normal and Emergency Conditions," PWRD-8-4, October 1993, pp. 2002-2008.

Roytelman, I., V. Melnik, S. S. H. Lee and R. L. Lugtu, "Multi-Objective Feeder Reconfiguration by Distribution Management System," *IEEE Transactions on Power Systems,* 11-2, May 1996, pp. 661-667.

Salama, M. M. A. and A. Y. Chikhani, "A Simplified Network Approach to the VAR Control Problem for Radial Distribution Systems", *IEEE Transactions on Power Delivery,* 8-3, July 1993, pp. 1529-1535.

Salama, M. M. A., E. A. A. Mansour, A. Y. Chikhani and R. Hackam, "Control of Reactive Power in Distribution Systems with an End-Load and Varying Load Condition", *IEEE Transactions on Power Apparatus & Systems,* 104-4, April 1985, pp. 941-947.

Salama, M. M. A., A. Y. Chikhani and R. Hackam, "Control of Reactive Power in Distribution Systems with an End-Load and Fixed Load Condition", *IEEE Transactions on Power Apparatus & Systems,* 104-10, October 1985, pp. 2779-2788.

Sarfi, R. J., M. M. A. Salama and A. Y. Chikhani, "Distribution System Reconfiguration for Loss Reduction: An Algorithm Based on Network Partitioning Theory," *IEEE Transactions on Power Systems,* 11-1, February 1996, pp. 504-510.

Sarma, N. D. R., V. C. Prasad, K. S. Prakasa Rao and V. Sankar, "A New Network Reconfiguration Technique for Service Restoration in Distribution Networks", *IEEE Transactions on Power Delivery*, 9-4, October 1994, pp. 1936-1942.

Sarma, N. D. R., S. Ghosh, K. S. Prakasa Rao and M. Srinivas, "Real Time Service Restoration in Distribution Networks - A Practical Approach", *IEEE Transactions on Power Delivery*, 9-4, October 1994, pp. 2064-2070.

Scott, W. G., "Automating the Restoration of Distribution Services in Major Emergencies", *IEEE Transactions on Power Delivery*, 5-2, April 1990, pp. 1034-1039.

Shirmohammadi, D., H. W. Hong, A. Semlyen and G. X. Luo, "A Compensation-Based Power Flow Method for Weakly Meshed Distribution and Transmission Networks", *IEEE Transactions on Power Systems*, 3-2, May 1988, pp. 753-762.

Shirmohammadi, D. and H. W. Hong, "Reconfiguration of Electric Distribution for Resistive Line Loss Reduction", *IEEE Transactions on Power Delivery*, 4-2, April 1989. pp. 1492-1498.

Shirmohammadi, D., "Service Restoration in Distribution Networks via Network Reconfiguration", *IEEE Transactions on Power Delivery*, 7-2, April 1992, pp. 952-958.

Smith, H. L., "DA/DSM Directions," *IEEE Computer Applications in Power*, 7-4, October 1994, pp. 23-25.

Stankovic, A. M. and M. S. Calovic, "Graph Oriented Algorithm for the Steady-State Security Enhancement in Distribution Networks", *IEEE Transactions on Power Delivery*, 4-1, January 1989, pp. 539-544.

Sun, D. I., S. Abe, R. R. Shoultz, M. S. Chen, P. Eichenberger and D. Farris, "Calculation of Energy Losses in a Distribution System", *IEEE Transactions on Power Apparatus & Systems*, 99, July/August 1980, pp. 1347-1356.

Sundhararajan, S. and A. Pahwa, "Optimal Selection of Capacitors for Radial Distribution Systems Using a Genetic Algorithm", *IEEE Transactions on Power Systems*, 9-3, August 1994, pp. 1499-1507.

Tang, Y., "Power Distribution System Planning with Reliability Modeling and Optimization," *IEEE Transactions on Power Systems*, 11-1, January 1996, pp. 181-189.

Taylor, T. and D. Lubkeman, "Implementation of Heuristic Search Strategies for Distribution Feeder Reconfiguration", *IEEE Transactions on Power Delivery*, 5-1, January 1990, pp. 239-246.

Tram, H. N. and D. L. Wall, "Optimal Conductor Selection in Planning Radial Distribution Systems", *IEEE Transactions on Power Systems*, 3-1, February 1988, pp. 200-206.

Ucak, C. and A. Pahwa, "An Analytical Approach for Step-by-Step Restoration of Distribution Systems Following Extended Outages", *IEEE Transactions on Power Delivery*, 9-3, July 1994, pp. 1717-1723.

Vanderplaats, G., *Numerical Optimization Techniques for Engineering Design: With Applications*, McGraw-Hill, 1983.

Wall, D. L., G. L. Thompson and J. E. D. Northcote-Green, "An Optimization Model for Planning Radial Distribution Networks", *IEEE Transactions on Power Apparatus & Systems*, 98-3, May/June 1979, pp. 1061-1068.

Wang, J.-C., H.-D. Chiang and G. R. Darling, "An Efficient Algorithm for Real-Time Network Reconfiguration in Large Scale Unbalanced Distribution Systems," *IEEE Transactions on Power Systems*, 11-1, February 1996, pp. 511-517.

Williams, B. R. and D. G. Walden, "Distribution Automation Srategy for the Future: Changing the Momentum," *IEEE Computer Applications in Power*, 7-3, July 1994, pp. 16-21.

Willis, H. L. and J. E. D. Northcote-Green, "Comparison of Several Computerized Distribution Planning Methods", *IEEE Transactions on Power Apparatus & Systems*, 104-1, January 1985, pp. 233-240.

Willis, H. L., R. W. Powell and T. D. Vismor, "A Method of Automatically Assessing Load Transfer Costs in Substation Optimization Studies", *IEEE Transactions on Power Apparatus & Systems*, 104-10, October 1985, pp. 2771-2778.

Willis, H. L., H. N. Tram and R. W. Powell, "A Computerized, Cluster Based Method of Building Representative Models of Distribution Systems", *IEEE Transactions on Power Apparatus & Systems*, 104-12, December 1985, pp. 3469-3474.

Willis, H. L., H. Tram, M. V. Engel and L. Finley, "Optimization Applications to Power Distribution," *IEEE Computer Applications in Power*, 8-4, October 1995, pp. 12-17.

Willis, H. L., H. Tram, M. V. Engel and L. Finley, "Selecting and Applying Distribution Optimization Methods", *IEEE Computer Applications in Power*, 9-1, January 1996, pp. 12-17.

Wood, A. J. and B. F. Wollenberg, *Power Generation, Operation and Control*, John Wiley and Sons, September 1979 (pre-publication version).

Vita

Thomas E. McDermott was born in St. Louis, Missouri in 1958. After receiving the Rensselaer Medal in high school, he attended Rensselaer Polytechnic Institute in Troy, New York. In 1980, he received the Bachelor of Science Degree in Electric Power Engineering from Rensselaer. He continued in Rensselaer's graduate school as an IEEE Fortescue Fellow, receiving the Master of Engineering Degree in Electric Power Engineering in 1981. While at RPI, he completed three cooperative education assignments at American Electric Power in New York City and in St. Joseph, Michigan. His first professional experience was at Westinghouse Electric Corporation's Advanced Systems Technology Division in Pittsburgh, Pennsylvania. At Westinghouse, he conducted staged switching surge tests and transient simulation studies using the Electromagnetic Transients Program. After Westinghouse sold the division to ABB, he worked at Power Technologies, Inc., also in Pittsburgh. There, he developed lightning protection design software for the Electric Power Research Institute, and performed a number of other consulting projects in electric power systems. He has also worked at Ansoft Corporation in Pittsburgh, developing commercial software for time-domain simulations of electromechanical devices based on finite element models. Since April 1997, he has worked for Electrotek Concepts of Knoxville, Tennesee, based at a home office in Pittsburgh. His projects at Electrotek focus on distribution planning and electrical power quality. In January 1994, he was admitted to the Ph.D. program at Virginia Tech, where he worked under the supervision of Dr. Robert Broadwater in electric power distribution system planning, design, and simulation. Mr. McDermott's areas of technical interest include distribution system planning, time-domain simulation of electrical circuits, and custom software development.

Publications

Cole, W. H. and T. E. McDermott, "A Computer Study and Model Demonstration of Safety Ground Locations During High Voltage Line Maintenance," *IEEE Transactions on Power Apparatus & Systems*, vol. PAS-103, no. 3, pp. 455-462, March 1984.

McDermott, T. E. and S. F. Mauser, "Digital Computer Simulation of Electromagnetic Transients in the Power Industry," *Society for Computer Simulation Conference*, Norfolk, VA, April 1984.

Frick, T. H., J. R. Stewart, A. R. Hileman, C. R. Chowaniec and T. E. McDermott, "Transmission Line Insulation Design at High Altitude," *IEEE Transactions on Power Apparatus & Systems*, vol. PAS-103, no. 12, pp. 3672-3680, December 1984.

Abi-Samra, N. C., R. F. Smith, T. E. McDermott and M. B. Chidester, "Analysis of Thyristor-Controlled Shunt SSR Countermeasures," *IEEE Transactions on Power Apparatus & Systems*, vol. PAS-104, no. 3, pp. 584-597, March 1985.

Bhasavanich, D., T. E. McDermott, D. M. Milone, J. S. Barnick, L. S. Frost and C. F. Kropp, "Digital Simulations and Field Measurements of Transients Associated with Large Capacitor Bank Switching on Distribution Systems," *IEEE Transactions on Power Apparatus & Systems*, vol. PAS-104, no. 8, pp. 2274-2282, August 1985.

Broadwater, R. P., J. C. Thompson and T. E. McDermott, "Pointers and Linked Lists in Electric Power Distribution Circuit Analysis," *IEEE PICA Conference Proceedings*, Baltimore, pp. 16-21, May 1991.

Elkins, D. L., A. C. Jain, T. E. McDermott and V. Rees, "Transients During 138-kV SF6 Breaker Switching of Low Inductive Currents," *IEEE Transactions on Industry Applications*, vol. IAS-29, no. 4, pp. 721-726, July/August 1993.

McDermott, T. E., T. A. Short and J. G. Anderson, "Lightning Protection of Distribution Lines," *IEEE Transactions on Power Delivery*, vol. PWRD-9, no. 1, pp. 138-152, January 1994.

McDermott, T., P. Zhou, J. Gilmore and Z. Cendes, "Simulation Models Magnets that Move," *Machine Design*, pp. 79-85, December 14, 1995.

McDermott, T., S. Hess and Z. Cendes, "A New Approach to Using Finite Element Solutions in System Simulation," *International Symposium on Automotive Technology and Automation*, paper 96VR006, Florence, Italy, June 1996.

McDermott, T., P. Zhou, J. Gilmore and Z. Cendes, "Electromechanical System Simulation with Models Generated from Finite Element Solutions," *IEEE Transactions on Magnetics*, vol. MAG-33, no. 2, pp. 1682-1685, March 1997.

Zhou, P., T. McDermott, Z. Cendes and M. Rahman, "Steady State Analysis of Synchronous Generators by a Coupled Field-Circuit Method," paper TA1-3, *IEEE International Electric Machines and Drives Conference Proceedings*, May 18-21, 1997, Milwaukee.